Doctoral Dissertation

Study on a gene network underlying sex spectrum of *Daphnia magna* by visualization and modification of *Dsx1* activity

Nong Dang Quang

August 2020

Biotechnology Global Human Resource Development Program

Department of Biotechnology

Graduate School of Engineering

Osaka University

CONTENTS

CHAPTER 1: INTRODUCTION

1.1 Sexual dimorphism and intersex

Almost all known animals on earth reproduce sexually [1] (also see [2] for exceptions). **Sexual reproduction** involves the recombination of two gametes, one created by mother and the other by father, to form a progeny inheriting genetic information from both. Basically, **female and male** are defined by the type of gamete they produce, in which male produces small and highly motile sperms while female produces large and non-motile ova.

Female and male of the same species are always physically different, at least at the reproductive organs (gonads, genitals…). This difference, known as **sexual dimorphism**, can also be found in various non-gonadal somatic traits as well as in behavior. In many cases, sexual dimorphism is so extreme that it makes male and female look like two unrelated species [3]. As a result, sexual dimorphism has become a standard (that people use) to assume the reproduction role of each individual in the population and categorize them into either female or male. This is called **sex binarism**.

However, the rule of dimorphism does not always prevail. To date, there have been numerous records of individuals that cannot be classified as male or female across various animal groups ranging from crustaceans [4], insects [5], birds [6], fish [7], to mammalians [8] including human [9,10]. Such individuals are either sexually mosaic, meaning male and female characteristics of any categories (morphology, gonad or even behavior) coexist in the same body, or in other cases are intermediate uniformities between male and female (Figure 1.1A). This seemingly natural existence of sexual ambiguities in any animal populations implies that the binary view of sex needs to be revised (Figure 1.1B, C) [11].

Sexual phenotypes deviating off the typical male and female scope can be the result of particular genetic and/or non-genetic conditions. Experimentally in nematode and fly, and clinically in human, numerous variations of untypical sexual characteristics caused by small mutations have been documented [12–14].

Figure 1.1: Binary and spectrum view of sex. (A) Examples of intersex animals. From left to right: Diana fritillary butterfly (*Speyeria diana*): Females are typically black with blue patterns, while male are smaller with brown and orange colorings. In the middle photo is an individual with bilateral gynandromorphism, meaning that left and right half of the body exhibits opposite sexual characteristics. Evening grosbeak (*Hesperiphona vespertina*): Male and female of this bird species are different in plumage. In particular, males have yellow belly while that of females is white. In the middle photo is also a case of bilateral gynandromorphism. Lion (*Panthera leo*): The mane is an exclusive feature of male lions. Dimorphism is also visible at the genitals. In the middle photo, a maned female is showing her back side revealing the vulva. White-tailed deer (*Odocoileus virginianus*): The well-developed and branching antlers is a trait that can only be found in male deer. The middle photos shows a female with her undeveloped velvet antlers. **(B)** The conventional binary view of sex. Following this view, there are only two categories of sex, male and female. Thus, intersexes are regarded as abnormalities and outliers of the population. **(C)** The contemporary concept of sex spectrum. In this model, sex occurs in a bimodal distribution with two peaks representing typical male and female and there is an overlap region demonstrating that intersexes are less common but as well an essential part of the population.

Photo source:
https://www.pinterest.de/pin/227361481162887104/
https://blog.lauraerickson.com/2019/03/abnormal-plumage-part-i-bilateral.html
https://www.pickpik.com/lion-lioness-predator-cat-wildcat-animal-world-133431
https://news.mongabay.com/2012/10/picture-of-the-day-the-maned-lioness/
https://en.wikipedia.org/wiki/White-tailed_deer
https://twitter.com/UtahDWR/status/1146095740659228672

External factors also alter sexual development of various, or possibly all, species, which will be described in later parts. To address sexual ambiguities without regard for the underlying cause, a neutral umbrella term, "**intersex**," is often used.

Intersex encompasses numerous variations of sexual characteristics, suggesting that there are much more than just male and female in nature, or in another word, **sex is a spectrum** (Figure 1.1C).

1.2 Role of genetic and environmental cues in sexual development

Sexual development includes two major processes: sex determination and sex differentiation [15]. **Sex determination** can be described as the series of molecular/cellular events that leads to the specification of sex for each individual and takes place before any morphological dimorphism can be detected. **Sex differentiation** subsequently occurs after the determination stage, involving the creation of sex-specific traits corresponding to the outcome of sex determination.

Sex determining mechanisms are greatly diverse, almost to the point that each species is seemingly trying to evolve their own way of deciding sex [16]. However, considering the nature of initial cues that trigger the cascade, all systems can be broadly divided into two categories: **genetic sex determination** (**GSD**) and **environmental sex determination** (**ESD**). GSD consists of species of which genotype will determine sexual identity of the animal. Male and female of GSD species are different right in their genetic constitution. A classic example is the male heterogamety (XY) system found in mammalian, *Drosophila*, etc., where females are homozygous (XX) and males are heterozygous (XY) at the sex chromosome pair (Figure 1.2). Similarly, in the female heterogamety (ZW) system found mainly in birds and some other species, females are heterozygous (ZW) and males are homozygous (ZZ), also at the sex chromosome pair. At least six other systems have been described in the GSD category. Species of ESD, on the other hand, rely on environmental factors to choose their sexual fate. For example, the eggs of turtles and some other reptiles hatch into either female or male depending on incubation temperature (temperature dependent system). Larvae of the spoon worm *Bonellia viridis*, upon landing onto female's proboscis, recognize a chemical secreted by the female as a masculinizing signal (chemical dependent system) [17]. In a social group of clown fish (subfamily Amphiprioninae), a dominant female, which is always largest in size, is

accompanied by a mature male and undifferentiated juveniles. When the female dies, her male partner ascends in social rank and undergoes sex change to become female. The largest in the remaining members turns into mature male to complete the breeding pair (social hierarchical dependent system) [18].

Similarly, an amazing diversity is also found in the mechanism of sex differentiation. All species reproducing sexually possess at least several sex-limited traits that is not only unique but sometimes also very elaborate, making sex traits one of the most fascinating and unpredictable phenomenon in the living world. These traits can be divided into three classes: primary (anatomical and physiological characteristics that are involved directly in sexual reproduction), secondary (body modifications and behaviors that contribute to reproductive success), and ecological (dimorphic traits related to ecological niche such as habitat use and diet) [3]. In order to relay sex information from the determination stage to the differentiation stage to initiate the building of various sexual dimorphic traits around the body, generally there are two methods: **cell-autonomous** and **non-cell-autonomous**. Cell-autonomous regulation of sex refers to the ability of each cell to know its own sex identity independently of external signals. Sex determination pathway is initiated by elements presenting inside the cell (a gene, genetic balance, or other inherited factors…) and directly dictates the outcome of sex differentiation. This mechanism is well described in GSD insects, for which gynandromorphs (individuals that are half male and half female due to mosaicism of genotype) serve as powerful evidence. Non-cell-autonomous regulation, on the contrary, is when a cell has to rely on exogenous information to learn its sex and differentiate correspondingly. For example, most vertebrates use sex-specific hormones, which are typically produced by the gonads, to transform tissues around the body. Tissues carrying matching receptors will differentiate accordingly to the hormone they receive regardless of their genotype, and the same tissue may take form of another sex if it is exposed to the other hormone. Interestingly, accumulating data suggest that, animals do not depend exclusively on only one method, but use both cell-autonomous pathway and non-cell-

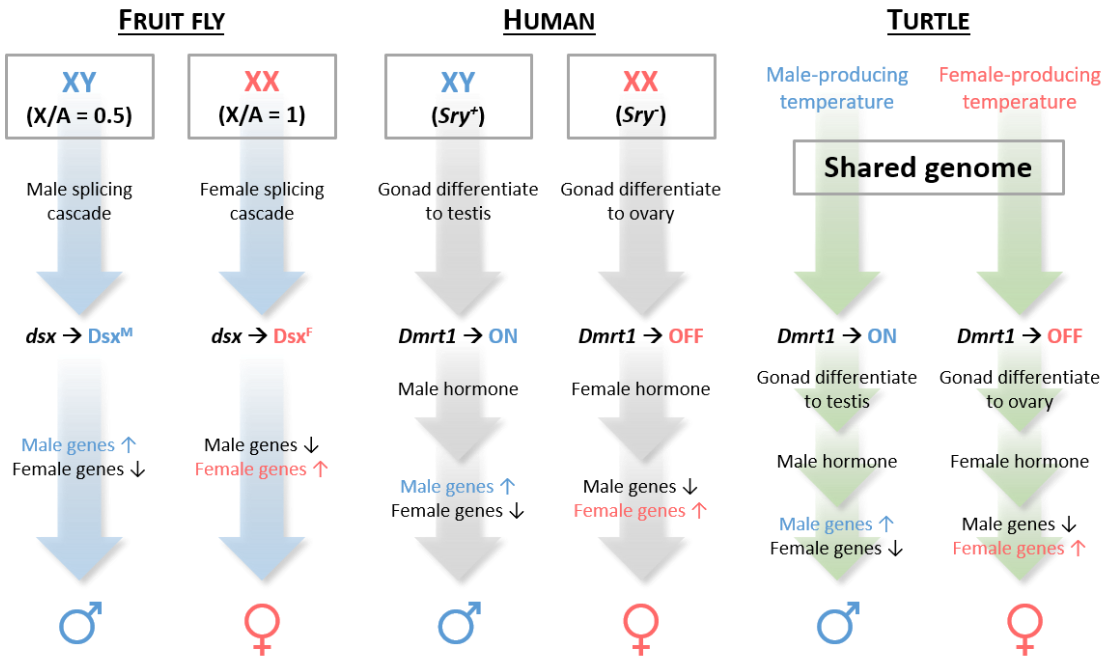

Figure 1.2: Molecular basis of sexual development. The well-documented pathways of fruit fly, human and turtle are shown in simplified diagrams. Fruit fly and human are GSD species with distinct genotypes for male and female. However, each fruit fly cell can typically initiate the cascade to determine its sexual fate by itself (cell-autonomous), while human cells require hormonal signal from the gonad to do the same thing (non-cell-autonomous). Eggs of turtle relies on incubation temperature to decide their sex and they also utilize sex hormones like most vertebrates. In all three cases, the role of a DM-domain gene as a binary switch of sex determination has been confirmed.

autonomous pathway to regulate sexual development of each tissue differently [19].

Thus, it can be seen that at cellular level, **sex is not a product of genetic makeup alone but also influenced by the environment**. This theory is strengthened by a number of studies which discovered that external factors such as temperature or bacterial infection can alter the sex of many insects [20,21]. Fish is also an animal group whose sex is plastic and subjected to changes in temperature, pH, hypoxia, population density, etc [22,23]. For animals utilizing sex hormones like most vertebrates, although the sex determination cascade is strictly controlled genetically, they are very sensitive to hormone analogs and

endocrine disrupting chemicals (EDCs) that may present in their surroundings and end up developing phenotypes that are inconsistent with their genotypic sex [24]. In species with high level of socialization such as human, social environment is also another factor that may directly interfere with the dimorphism of behavior and emotions, which in turn potentially affects sexual development [25].

Because of this complexity in the creation of sex, a contemporary concept has emerged that sex is not essentially binary or completely encoded in the genome, but rather a product of the interaction between genome and environment and may take any form in a continuum. Thus, it would be inappropriate to just base on one single aspect, for example karyotype or certain physical traits, to draw a conclusion about the sexual identity of an individual. To correctly interpret the nature of sex, it is crucial to establish a complete and quantifiable set of molecular markers.

1.3 DM-domain gene: A conserved sex determining factor

Accumulating studies into the molecular basis of sexual development have revealed that, despite the great diversity at the top of sex determination cascade and heavily branching of sexual differentiation mechanisms, a common node can be found at the connecting point of the two processes where the Dsx/Mab-3 (DM) domain gene family is involved [26,27]. Originally identified in *Drosophila* through a mutation causing the animal to develop as intersexes, the involving gene was named *doublesex* (*dsx*) [28]. Later, also through a mutant, another gene named *male abnormal-3* (*mab-3*) was found to be essential for male-specific functions in *Caenorhabditis elegans* [29]. Surprisingly, *Caenorhabditis mab-3* and *Drosophila dsx* share a similar DNA-binding motif which was then referred to as Dsx/Mab-3-domain (DM-domain). Henceforth, transcription factors containing DM-domain have been identified from various invertebrates and vertebrates including mammals, making up a conserved gene family that is important not only in sex determination but also in other developmental processes.

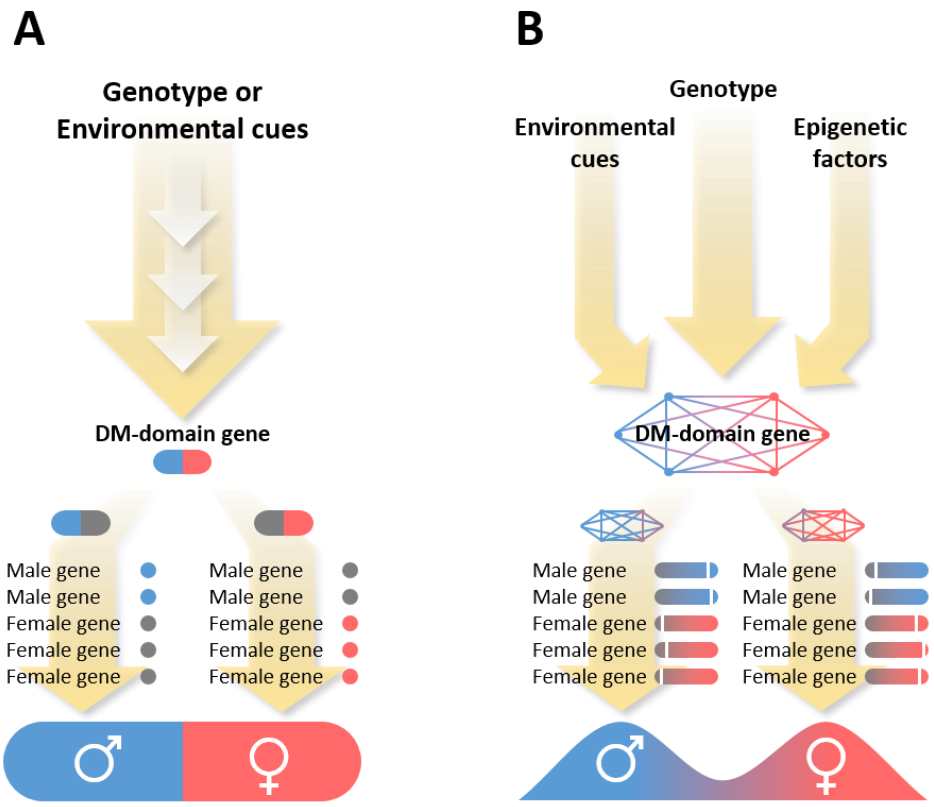

Figure 1.3: Two models of sexual development. (A) The classic model. A particular signal, which is genotype for GSD species or environmental cues for ESD species, is required to initiate the sex determination cascade. Signal is relayed in a linear manner and stabilized through a series of hierarchical elements until it reach the bottom where a binary switch (for example a DM-domain gene) can be found. Depending on the state of this switch, downstream sex differentiation genes are turned on or off correspondingly, ultimately shaping the sex of the body. This model is supported by molecular data from many species, but cannot explain intersexuality well. **(B)** A newly proposed model. For all species, not a single cue but various signals including genotypic, epigenetic and environmental information will contribute as input for sex determination. Also, endpoint of sex determination cascade is not a single master switch but rather a cassette of interactive genes in which the DM-domain gene is likely a core member. Equilibrium of this cassette, which varies between masculinizing and feminizing state, will dictate the activity of downstream sex differentiation gene in a tunable fashion, thus creating a continuum of sexual phenotypes, i.e. sex spectrum.

Binary activity of DM-domain genes, either in alternative-splicing style or on/off style, was found to play an important role in regulating the sexual development of many species (Figure 1.2). The alternative-splicing style is found in insects, in which the DM-domain gene *doublesex* can be spliced in to either

male of female isoforms and each version will in turn promote the differentiation into one sex and repress the opposite [30]. The on/off style is found in many other species including mammalians, birds, reptiles, fish, and nematode… where activation of DM-domain genes generally results in male differentiation [31–33]. Although different animal groups recruit very different machineries to initialize and control the activity of this gene, stabilizing its binary state seems to be the common theme, suggesting that binarism of the sex-determining switches is the mastermind behind sexual dimorphism.

However, unlike genes in the sex-determination cascade, those of sexual differentiation network which directly give rise to sexual traits do not seem to follow the binary law. Many dimorphic characteristics, for example body size, muscle mass or even circulating hormonal level, are quantitative traits which is affected by both genetic and environmental factors and usually display overlap between male and female, i.e. in a bimodal distribution [34]. Interestingly, it was reported in *D. melanogaster* that intersex phenotypes could be obtained from *dsx* mutants in which this gene was completely or partially disrupted [35]. Also, mammalian *dmrt1* was found to be dosage-sensitive in its role in male gonad differentiation [36]. These data suggest that despite being important, binary action of sex determining switches like the DM-domain gene alone is insufficient for dictating the outcome of sex. Although sex determination cascade is conventionally regarded as a linear signaling cascade of hierarchical elements where DM-domain gene usually stays around the bottom position, in newly emerged perspectives, it is recognized that there is no single bottom switch. Instead, there must be an interactive sex determining cassette with multiple signal entries and the equilibrium state of members in this complex cassette will decide the sexual fate of each individual (Figure 1.3) [37]. Nevertheless, since the DM-domain genes is a core member, investigation into this gene in order to get a hold of its surrounding factors is an important work.

1.4 *Daphnia* as a model organism for the study of sex

The water flea *Daphnia* sp. is a genus of planktonic crustacean populating fresh and brackish water worldwide. Being not only a popular source of fish food in aquariums, species of *Daphnia* genus have been used in biological research since the 18th century [38].

There are many features of *Daphnia* sp. that attract researchers. First, they belong to the Cladocera order of Branchiopoda class which appeared on earth from as early as the Devonian period and is one of the first dwellers of fresh water environment [39]. Recent morphological and molecular evidence shows that branchiopods are closely related to insects (which has resulted in the grouping of Crustacea and Hexapoda into one single clade named Pancrustacea) and appear to be more similar to their common ancestor, making them a particularly antique group of animals [40,41]. Second, by grazing mainly on phytoplankton such as unicellular algae, daphniids together with rotifers and copepods make up a critical node in the food web of the earth ecosystem [42]. As a major primary consumer and prey to a wide range of predators, changes in *Daphnia* populations have great impact on the environment and are recognized as an indicator of aquatic ecosystem's health. The *Daphnia* microbiota, which symbiotically support the animal's welfare and help assimilate the energy from their high-fiber diet, are also among the most intriguing ones with several host-exclusive interactions [43–47]. Last but not least, *Daphnia* is well known for their ecoresponsive characteristics, meaning that they are not only fragile and highly sensitive to changes in the surroundings but also can develop alternative phenotypes to adapt to the situation. Cyclomorphosis, i.e. seasonal change in morphology through successive generations, is a signature ability of *Daphnia* in which some species can grow bulky helmets or crests while others can elongate their neck teeth or tail spines during heavy predation season. This transformation can be triggered by abiotic factors such as temperature, light and water turbulence [48], or by biotic factors such as food condition and kairomones released by predators [49]. Cyclomorphosis has been proven to be a defensive mechanism to increase the

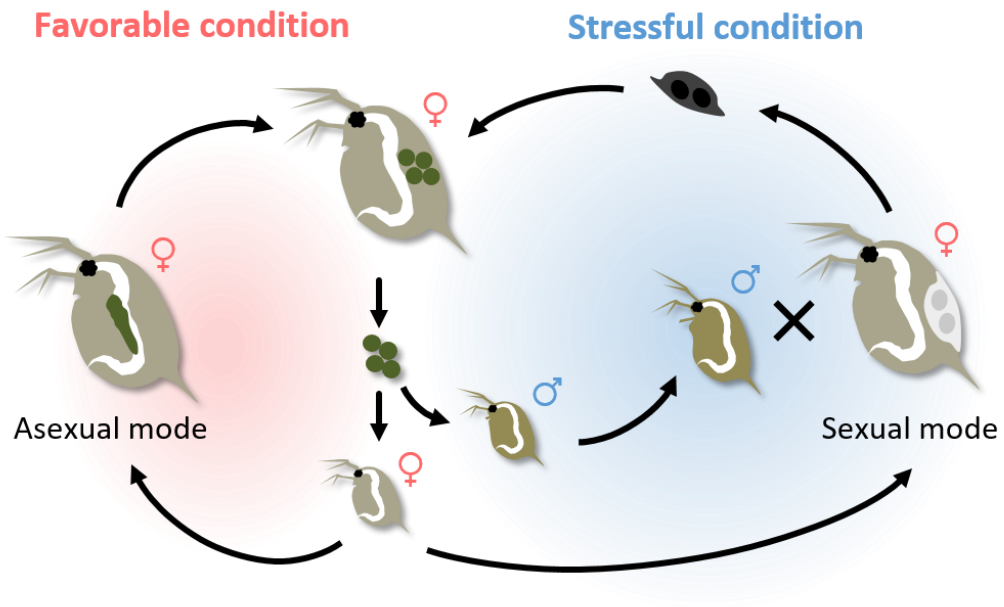

Figure 1.4: Life cycle of *Daphnia magna*.

survival rate of the population [50,51]. As a rare case of crustacean that use hemoglobin for respiration [52], the hemoglobin level in daphniid's hemolymph can also increase drastically under hypoxia to maximize oxygen transportation, turning the body red [53]. Other life history traits of daphniids such as survivorship, growth and fecundity also sensitively fluctuate in response to a wide range of chemicals [54], making them a standard model for toxicity tests that is specified in two tests of the OECD (Organisation for Economic Co-operation and Development) Guidelines for the Testing of Chemicals [55,56].

Surprisingly, reproduction of *Daphnia* is as well another trait that is profoundly ecoresponsive. Between seasons, *Daphnia* population alternatively switches between asexual and sexual mode of reproduction and this unique ability is called cyclic parthenogenesis (Figure 1.4) [57]. In details, during growth season when living conditions are optimal, mother daphniids produce clonal daughters asexually in large quantity (dozens per mother per clutch), quickly expand the size of their population. However, when food becomes scarce and temperature or daylight is not favorable anymore (typically when winter comes), from the crowded and stressful population, clonal males appear, followed by females starting to

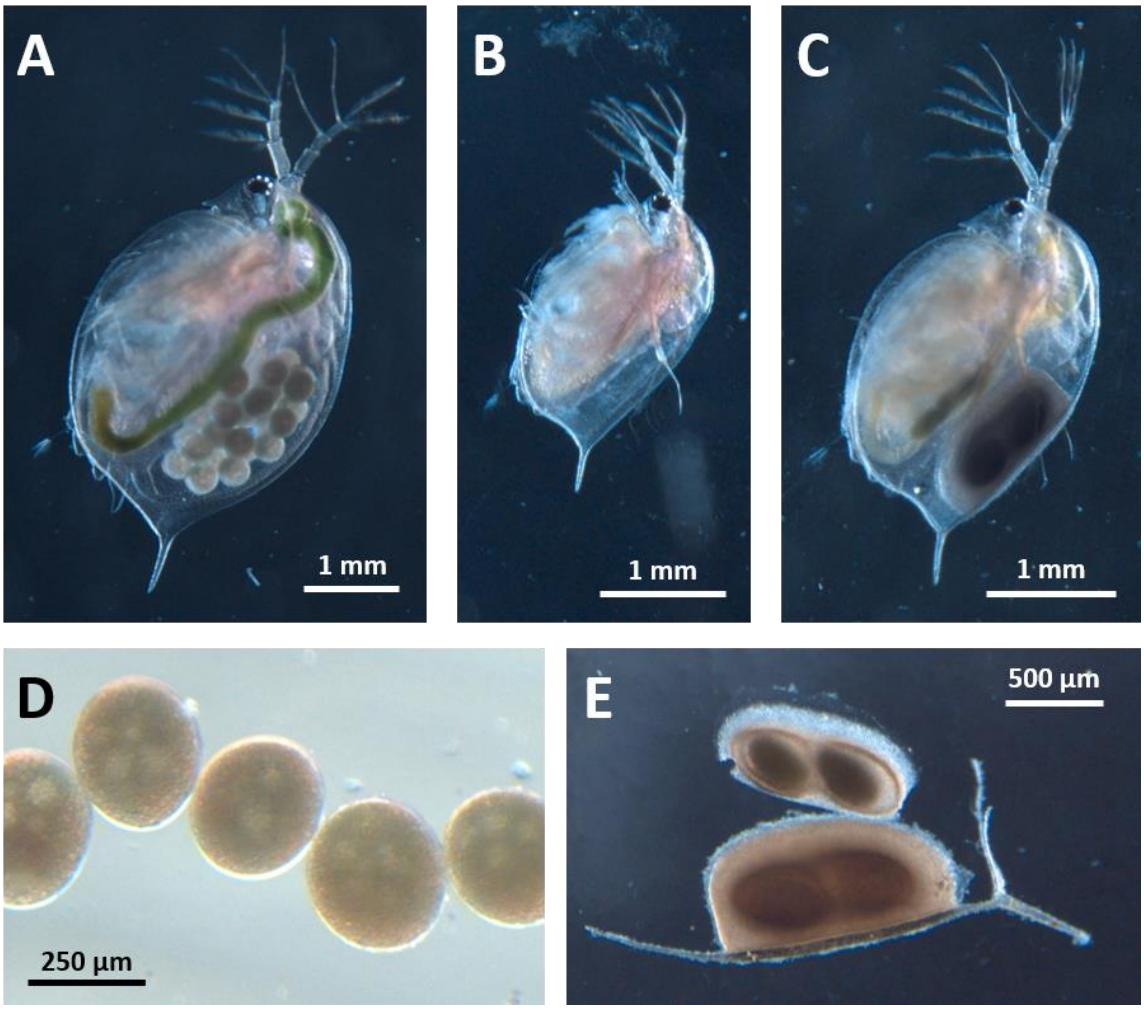

Figure 1.5: Photos of *Daphnia magna*. (A) An adult female carrying asexual eggs. **(B)** An adult male. **(C)** An adult female carrying an ephippium. **(D)** Some developing asexual eggs. **(E)** An ephippium with outer shell, inner case and two deposited resting eggs.

produce haploid eggs that need fertilization. Mating occurs and results in the production of resting eggs that are deposited into protective shells known as ephippia [58–61]. Resting eggs are produced in limited quantity (maximum two per mother per clutch) but they are extremely tolerance against dehydration, heat/cold and even erosive chemicals [62–64]. These eggs undergo dormancy as a way to escape the harsh environment and will hatch when favorable conditions return. However, in nature, a large proportion of resting eggs do not hatch and get buried into the sediment of lakes and ponds, serving as a valuable category of

fossils that can be resurrected [65–67]. In other words, the single *Daphnia* genome can express into multiple reproductive forms, either asexual female, sexual female or sexual male, all responsively to epigenetic factors, making them a very interesting model for the study of sex (Figure 1.5).

1.5 Molecular basis of sexual development in *Daphnia magna*

Daphnia magna is among the largest species of this genus with body length of adult female can measure up to 5 mm. In optimal condition, *D. magna* newborns will molt 4–5 times with 2-day interval to reach reproduction age. Mature females release 20–30 asexual eggs every 3 days and oviposition takes place shortly after each molting. Eggs are carried by mother inside the brood chamber and hatchlings will swim out around the next time the mother molts [57,58,68–70]. *D. magna* is considered to be very easy to handle due to desirable body size and fast life cycle. Maintaining them for laboratory use is also simple and low-cost. Other advantages include their transparent body which allows observation of inner tissues and clonal reproduction which allows easy control of a genetically homogeneous population. However, despite being used in biology research since very early, *D. magna* molecular genetics is rather lagged behind with their first full genome sequence released in 2010 [71], quite later than other model species.

Still, sexual development of *D. magna* has attracted numerous studies (Figure 1.6). It has long been known that sex determination in *D. magna* is not genotypic but relies on environmental cues [72]. Males are typically born in a stressful population (mentioned above) from the same kind of eggs as their sisters and no sex chromosome has been identified so far [73,74]. Previous studies discovered that male determination of daphniids is controlled by the crustacean juvenile hormone (JH) methyl farnesoate (MF) in which exposure of mothers to analogs of this hormone could induce part of or entire brood to develop into males independently of environmental conditions [75]. Later, it was found out that the sensitive window to juvenile hormone analogs for male determination of *D. magna* was very narrow, only 4–10 hours before oviposition while oocytes are still inside the ovary [76,77]. There is also evidence that female daphniids produce MF in

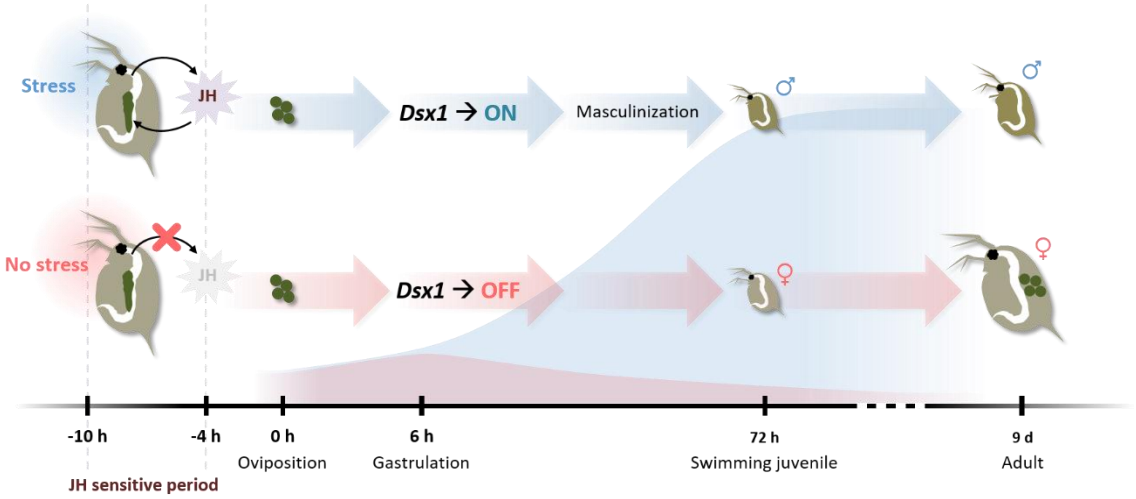

Figure 1.6: Mechanism of sexual development in *Daphnia magna*. The role of juvenile hormone (JH) as a male production inducer and *Dsx1* as the major masculinization factor is well documented. Other elements that interact with these two factors still remain elusive. Blue/red area in the background illustrates *Dsx1* expression level.

response to stress and the MF signaling is required for male production [78,79]. However, it is still unclear whether the developing oocytes respond directly to the external hormone or to some unknown maternal factors.

Upon exposure to JH analogs, activation of *Doublesex1* (*Dsx1*), a DM-domain gene of *D. magna*, in the developing male embryo has been reported. *Dsx1* transcripts present in freshly ovulated eggs (0 h) of both male and female at comparable amount, but exclusively increase in male after gastrulation (6 h) [80,81]. This dimorphic pattern persists until adulthood, and strong *Dsx1* expression can be found in male-specific tissues such as first antennae, copulation hooks and testes. Knock-down of *Dsx1* in male embryos led to feminization of gonadal and non-gonadal tissues, while ectopic expression of this gene in female embryos led to partial masculinization [80]. It was inferred from these data that *Dsx1* is the core masculinization factor in *D. magna* and probably positioned around the bottom of sex determination cascade as described in many other species. Still, upstream regulators that relay JH signal to *Dsx1* and downstream targets of this gene remains largely unknown.

1.6 Objective of this study

In this study, I aim to **clarify the nature of molecular cascade responsible for *D. magna* sexual development**. According to previous studies, by varying the exposure concentration of JH analogs, from the same brood mixtures of male and female newborns in different ratios can be obtained but intersexuality will not occur [82]. This suggest the robustness in maintaining the binary state of sex in *D. magna* despite unstable input signal. In contrast, there are records that intersex daphniids may appear in populations treated with high temperature [83], suggesting that *D. magna* individual sex must be plastic and responsive to various environmental cues. To resolve this contradiction at physiological level, I carried out an investigation into the underlying molecular pathway and this work includes three main parts:

1) A reporter strain that allows in vivo tracking of *Dsx1* activity was created by replacing one copy of *Dsx1* with a red fluorescence protein coding gene. Using this reporter, I demonstrated that the binary activity of *Dsx1* was maintained throughout daphniid lifespan, leading to the stabilization of dimorphic traits. This will be described in Chapter 2.

2) By directly mutating the *Dsx1* gene, mutants showing intersex phenotype were obtained. Transcriptomic analysis of the intersex daphniids revealed that a large proportion of *Dsx1* downstream genes functioned in a tunable rather than binary fashion. This will be described in Chapter 3.

3) Dsx1-active cells were isolated for comparison of gene expression with cells not expressing *Dsx1*. I could obtain evidence showing the asymmetry relationship between *Dsx1* and sex-nonspecific genes, suggesting that *Dsx1* does not dictate sex differentiation alone. This experiment is still ongoing and will be described in Chapter 4.

CHAPTER 2: GENERATION OF A *DSX1* REPORTER STRAIN

2.1 Introduction

To predict the function of a gene and how that gene interacts with others, understanding its spatio-temporal expression is very important. Although male-specific activity of *Dsx1* is well-demonstrated in *D. magna*, currently available data were acquired using qPCR and in situ hybridization, providing only snapshots of *Dsx1* activity [80]. In recent years, genome editing techniques are becoming more and more available. For *D. magna*, not only microinjection and electroporation platforms has already been established, successful loss- and gain-of-function manipulations using TALEN and CRISPR/Cas systems were also reported [84–94]. Therefore, to fill in the gap of unknown *Dsx1* behavior throughout development, creating a knock-in reporter strain that can visualize *Dsx1* expression would be the most reasonable approach.

To achieve this, a common method is to integrate a construct harboring a reporter gene (fluorescence coding gene for example) that is linked to the regulatory region of the gene-of-interest (promotor, etc.) into the genome. However in the case of *Dsx1*, no regulatory sequence has been documented. The *Dsx1* gene of *D. magna* spans a 20 kb genomic region but introns already occupy 80% of the gene length. Upstream intergenic region is about 0.5 kb, downstream intergenic region is about 7 kb and coding sequence (CDS) is 993 bp, meaning that the length of reporter cassette should be around 20–27 kb in order to ensure faithful recapitulation. As this is too long for molecular cloning as well as for currently available knock-in platforms, an alternative method was chosen. Since the CDS of *Dsx1* locates entirely inside the final exon of this gene, it is possible to replace *Dsx1* CDS with only the reporter gene so that the inserted reporter can be expressed under the endogenous regulatory context. This can normally be done by homologous recombination (HR). However, since efficiency of HR-mediated knock-in protocols in *D. magna* is still very low, another design that utilizes non-homologous end joining (NHEJ) was chosen.

In this chapter, I describe the generation of two mutants, namely Line A and Line B, by TALEN+NHEJ-mediated gene editing. Furthermore, I could validate one of them, Line B, to be a desirable reporter for *Dsx1* and use this line to create a detailed mapping of *Dsx1* spatio-temporal expression.

2.2 Materials and Methods

2.2.1 *Daphnia* strains and culture conditions

A wildtype strain of *D. magna* obtained from the National Institute for Environmental Studies (Tsukuba, Japan), namely NIES strain, together with a previously established transgenic strain of *D. magna* carrying two tandem copies of an EF1α-1::H2B-GFP construct [95], namely HG2E strain, were used in this study. In the HG2E strain, strong and ubiquitous expression of a H2B-EGFP fusion protein is driven by the *D. magna* EF1α-1 promoter/UTR cassette, resulting in a permanent green fluorescent signal that can be observed in cell nuclei throughout the animal body. This genetic background provides an easy definition of the animal's anatomy at every stage of development. For regular culture, daphniids were maintained as populations containing 80 females in 5 L ADaM medium [96]. Each population was fed daily with 1.12×10^9 *Chlorella vulgaris* cells, and new-born juveniles were removed regularly. The ambient temperature was kept at 22–24 °C and light/dark photoperiod was fixed at 16/8 h. For daphniids to be observed using fluorescence microscopy, the algae were replaced by dry yeast at 0.3 mg per daphniid per day to avoid autofluorescence.

2.2.2 Designing TALENs

The *Dsx1* locus in the host strain was previously sequenced independently in our laboratory (unpublished data). This sequence was used as the query sequence in the web-based tool TAL Effector Nucleotide Targeter (TALE-NT) 2.0 [97] using the following parameters: spacer length = 15–20, repeat array length = 15–20, G substitute = NN, Streubel et al. guidelines = On, upstream base = T only. A design potentially targeting immediately adjacent to the start codon of *Dsx1* ORF was chosen.

2.2.3 Construction of TALEN expression vectors

In order to assemble the full coding sequence of each TALEN (left and right) into a vector suitable for in vitro transcription, the Golden Gate method was used as previously described [98]. Briefly, at first, the RVD units were assembled onto the GoldyTALEN backbone, resulting in the generation of pT3TS-dsx1start-TALEN-left and -right. Subsequently, from these vectors, the DNA-binding domains were swapped with those from pCS-Dmavas-dsr-TALEN-left-ELD and -right-KKR, using a pair of restriction enzymes (XbaI and BsaBI) [88], leading to the final construction of pCS-Dmavas-dsx1start-TALEN-left-ELD and -right-KKR expression vectors.

2.2.4 In vitro transcription

To generate linear templates for in vitro transcription, the two TALEN expression vectors were first digested with Acc65I, and then subjected to purification using a QIAquick PCR purification kit (QIAGEN GmbH, Hilden, Germany). With these templates, capped-transcription was performed using the mMessage mMachine SP6 kit (Life Technologies, California, USA), followed by a tailing reaction using a Poly(A) Tailing kit (Life Technologies). After this, the products underwent a three-step purification using miniQuick Spin RNA columns (Roche Diagnostics GmbH, Mannheim, Germany), phenol/chloroform purification, and ethanol purification, before being dissolved in DNase/RNase-free water (Life Technologies).

2.2.5 Construction of donor vector

The donor vector consisted of three main elements: i) a recognition sequence for the designed TALEN pair (48 bp), ii) a full coding sequence of the red fluorescent protein-encoding gene *mCherry* (711 bp), and iii) a full-length sequence of *Dsx1* 3’ UTR cloned directly from the last exon of the host animal (2,458 bp). These elements were seamlessly assembled in the respective order onto the pRN3 backbone using the In-Fusion® HD Cloning Kit (Clontech), resulting in a 6,057 bp plasmid.

2.2.6 Microinjection

To introduce foreign materials one-cell embryos of *D. magna*, I followed a previously established microinjection-based protocol [85]. Briefly, freshly ovulated eggs from 2- to 4-week-old *Daphnia* mothers were retrieved. The eggs were then incubated in ice-cold M4-sucrose solution and microinjected using home-forged glass needles on a specialized trenched plate within 1 hour. The injection solution contained 500 ng/μL of each TALEN mRNA with or without 50 ng/μL of donor vector. Approximately 0.2 nL of the solution was injected into each egg. The injected eggs were then incubated in M4-sucrose for at least 3 days at 22–24 °C before being transferred to ADaM medium and cultured normally.

2.2.7 TALEN functionality test

TALENs were injected into *D. magna* embryos without the presence of the donor vector. After 72 h, each injected sample was collected separately and total genomic DNA was extracted. In-del mutations at the target site of TALENs were confirmed using the primer pair Dsx1_start_left and Dsx1_start_right that is designed to amplify a 186 bp region around the wild-type *Dsx1* start codon (see Table S1 for primer sequence). PCR products were separated on 20% polyacrylamide gel and stained with SYBR Green I.

2.2.8 Screening for G0 candidates

To screen for G0 candidates obtained by co-injection of TALEN mRNAs and the donor vector, all G0 daphniids that could survive until reproduction age were cultured separately, and germline transmission of the donor vector was analyzed using first clutch G1 offspring. Three PCR-based tests were carried out: i) the primer pair mCherry_check_F and mCherry_check_R, which amplified a 184-bp region within the mCherry CDS, was used to confirm the presence of donor vector in the genome, ii) the primer pair Dsx1_start_left and mCherry_check_R, which amplified a 729-bp region spanning the left junction of the expected genotype, was used to confirm the integration of the donor vector into the target site in the correct direction, and iii) the primer pair Dsx1_start_left

and Dsx1_start_right, which amplified a 186-bp region around the *Dsx1* start codon, was used to confirm the integrity of the other allele. G0s that were positive for all three tests were then selected as the founder animals. Information on these primers can be found in Table S1.

2.2.9 Genotyping of the knock-in candidates

At first, quantitative PCR was used to determine the copy numbers of donor vectors integrated into the host genome. The CDS of *mCherry* was targeted using the primer pair mCherry_qPCR_F and mCherry_qPCR_R (product size = 112 bp). The housekeeping gene encoding ribosomal protein L32, which has two copies in the *D. magna* genome, was used as the reference and targeted by the primer pair DmagRPL32-realtime-5 and DmagRPL32-realtime-3 (product size = 67 bp).

Next, regions susceptive to in-del mutations were amplified using specific primers: Seq_Dsx1Start_L and Seq_Dsx1Start_R for the non-inserted Dsx1 allele (TALEN target), Seq_mChVector_R (head) and Seq_mChVector_L (tail) for the Dsx1 promoter–vector junction (left junction), right_junc_6kb_L and right_junc_3kb_alt_R for the vector–Dsx1 ORF junction (right junction), and vect_connect_L and vect_connect_R for the vector–vector junction (vector connecting junction). The obtained fragments were cloned using the Zero Blunt® TOPO® PCR Cloning Kit (Thermo Fisher Scientific) and ultimately sequenced. Information on these primers can be found in Table S1.

2.2.10 Production of male daphniids and resting eggs

To induce the production of males from mother daphniids, a previously described method was used [76]. In short, 2- to 3 -week-old females were treated with 1 µg/L Fenoxycarb (Wako Pure Chemicals, Osaka, Japan) so that oocytes at sensitive stages (50–56 h of ovarian development) could be exposed to the chemical. All individuals of the oocyte clutch would later develop into males.

To induce resting egg production, males and females were kept together in a 1:7 ratio under a high population density and starving conditions. In details, 25 males and 175 females were cultured in the same beaker containing 1 L ADaM,

and fed with 4.2×10^8 *Chlorella* cells once a day. Females were expected to produce ephippia after 1 or 2 weeks. From each beaker, all collected ephippia were opened to retrieve the resting eggs inside. This was done by holding the two ends of ephippium with two pairs of forceps, then push together to pop the eggs out through the unseamed edge of the ephippium. Total ephippium count and total egg count were recorded. The frequency of fertilization = total egg count / (total ephippium count × 2).

2.2.11 qRT-PCR

Total RNA was extracted from sample triplicates and subjected to cDNA synthesis using random hexamers (Invitrogen). SYBR® GreenER™ qPCR SuperMix Universal Kit (Invitrogen) was used for qPCR, and reactions were conducted using an Mx3005 P Real-Time PCR System (Agilent Technologies, CA, USA). To amplify the common CDS of *Dsx1* transcripts, previously described primers [80] were used. To amplify the *mCherry* CDS, the mCherry_qPCR_F and mCherry_qPCR_R pair (Table S1) was used. To amplify the housekeeping L32 gene, the DmagRPL32-realtime-5 and DmagRPL32-realtime-3 pair (Table S1) was used.

2.3 Results

2.3.1 TALEN design and knock-in strategy

I chose a design of TALENs that was supposed to induce double strand break right in front of the start codon of *Dsx1* CDS (Figure 2.1). In this strategy, upon microinjection into the cytoplasm of newly ovulated eggs, the mRNA of TALENs would be translated into active proteins via endogenous translation machinery. Through binding onto the recognition sites, these nucleases would dimerize and digest the target, separating *Dsx1* CDS from its promoter. On the donor vector, the exact 46-bp recognition sequence of TALENs was placed directly at the upstream of *mCherry* coding sequence (Figure 2.2) so that the vector would also be linearized by the same design of TALENs. In my expectation,

A. Query sequence

5'-TGAAAAGAATCTAAACCCAATTGTTTTTTTGTTTTCTTTTCTCTCTGAAACATTAGGTGCTTTTCATTAGAC
ATCAATGTCAGATAGCGACGCTGAAGAATTGTCCGTGGGGGCACCGTCGCCGATTTCAGCTAAAGAGCGC-3'

(= exon, = *Dsx1* CDS)

B. The chosen design of TALEN pair

options_used:array_min = 15, array_max = 20, spacer_min = 15, spacer_max = 20, upstream_base = T									
Sequence Name	**Cut Site**	**TAL1 start**	**TAL2 start**	**TAL1 length**	**TAL2 length**	**Spacer length**	**Spacer range**	**Unique RE sites in spacer**	**% RVDs HD or NN/NH**
dsx1	120	97	142	16	15	15	113-127	DrdI:GACNNN NNNGTC	42
TAL1 RVDs	NG NI NN NN NG NN HD NG NG NG NG HD NI NG NG NI								
TAL2 RVDs	NG HD NG NG HD NI NN HD NN NG HD NN HD NG NI								
Plus strand sequence	T TAGGTGCTTTTCATTA gacatcaatgtcaga TAGCGACGCTGAAGA A								

Figure 2.1: TALEN design. (A) The short genomic sequence from *Dsx1* locus that was used as the query for designing of TALEN. **(B)** Description of the chosen design, extracted from the output result of TALE-NT 2.0 web-based tool.

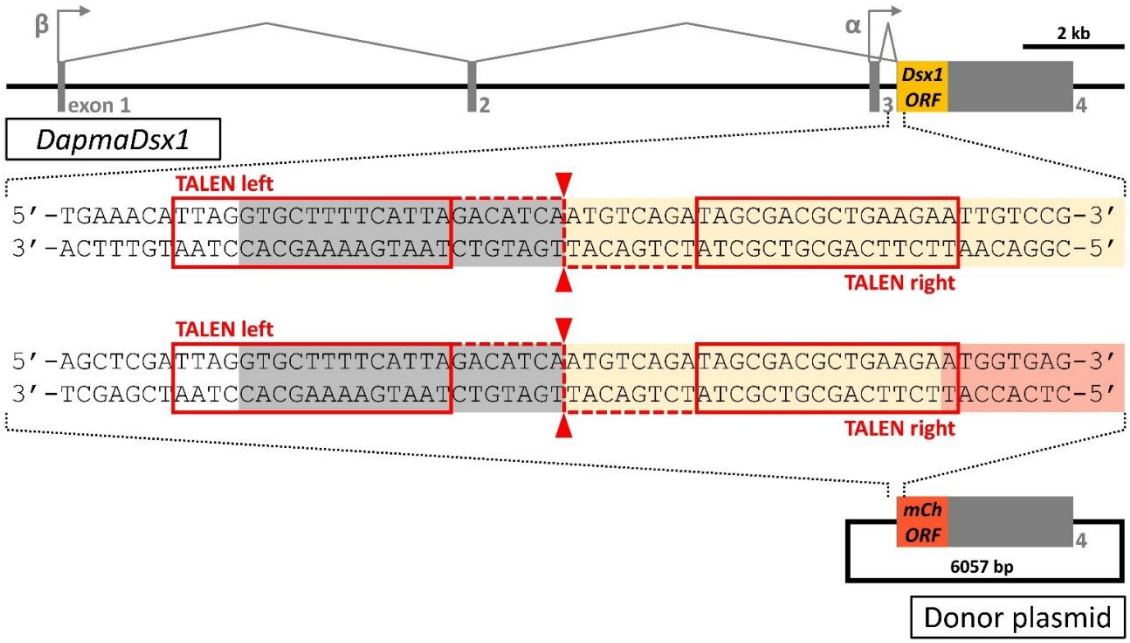

Figure 2.2: Knock-in strategy. There are two different promoters, alpha and beta, directing the transcription of two *Dsx1* transcripts which are different only in 5' UTR region. TALEN was designed to target a 46 bp sequence at the beginning of the common exon 4 which contains the full ORF of *Dsx1*.

a copy of the donor vector would be integrated into one of *Dsx1* alleles via the NHEJ machinery while another allele would remain intact. In the obtained genome,

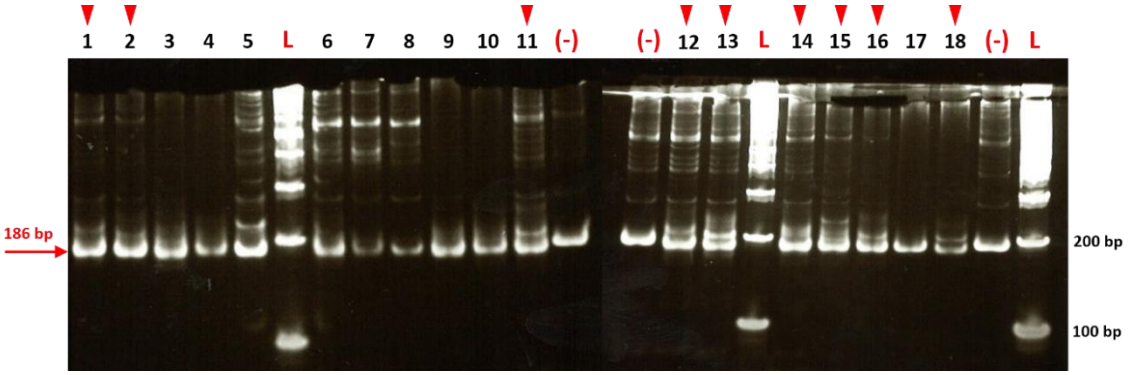

Figure 2.3: Functionality test of TALENs. Injection of only TALEN mRNAs caused a typical pattern of chimeric in-del mutation in the genome of the injected 72 h juveniles visible on 20% polyacrylamide gel. (-): genome samples from non-injected embryos. Red arrow heads: cases with very obvious multi-banding pattern, a sign of in-del mutation. L: DNA ladder. In this figure, of 18 tested embryos, 9 (50%) showed clear sign of in-del mutation, indicating a fairly high efficiency of the TALEN design.

mCherry should be regulated by the endogenous *Dsx1* promoter. Also, the full-length 3' UTR of *Dsx1* (which is supposed to participate in the regulation of this gene [80]) was put after *mCherry* to ensure a faithful mimicking of the reporter.

2.3.2 In vivo functionality of TALENs

Before being used for knock-in experiment, in vivo functionality of TALENs must be tested. TALEN mRNAs were injected into *D. magna* freshly ovulated asexual eggs and the presence of in-del mutation in the 72 h juveniles was checked by PCR. From 43 injected eggs, 18 were chosen randomly for the PCR test and as a result, in-del mutation was found in at least 9 cases (50%, Figure 2.3). Comparing to previous report, in which the inherited knock-out frequency was 80% for hemizygous target and 22% for homozygous target [88], the obtained efficiency was not particularly high. However, I decided that such efficiency is still feasible for further experiments.

2.3.3 Generation of two knock-in mutants, Line A and Line B

To generate knock-in candidates, coinjection of TALEN mRNAs and donor vector was performed. At first, founder animals were screened using a triple PCR test as described in Materials and Methods section. From 83 successfully injected

Injected solution	Injected eggs	72 h survivals	Adulthood survivals	Test 1 positive	Test 1+2 positive	Test 1+2+3 positive
TALEN mRNAs (500 ng/μL each) **+ vector** (50 ng/μL)	83	31/83	18/31	3/18	2/3	**2**/2
		37.3%	**58.1%**	**16.7%**	**66.7%**	**100%**

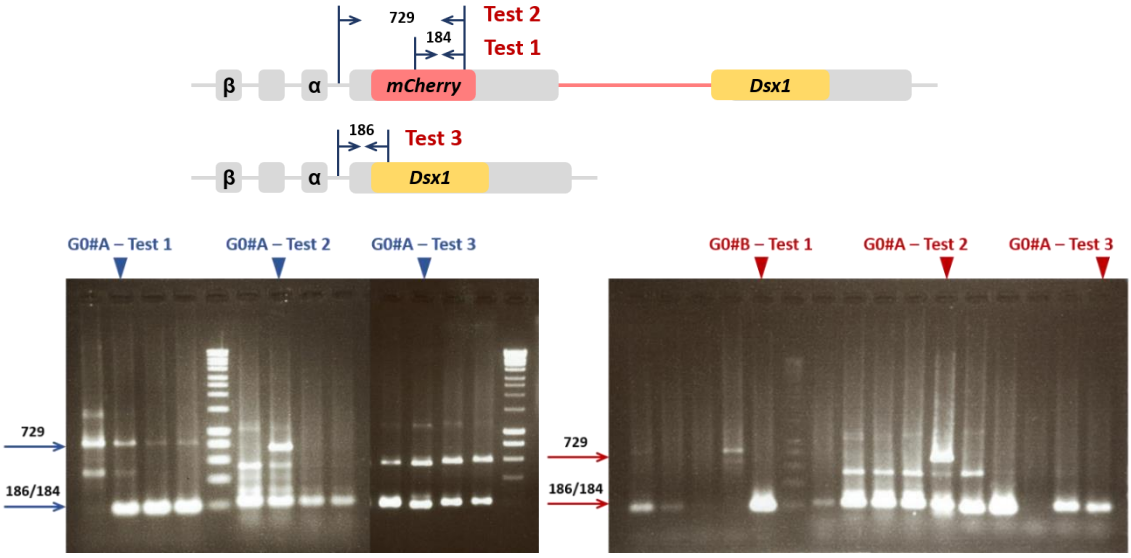

Figure 2.4: Microinjection and screening result for G0 candidates. From 83 injected embryos, two were found to be positive for all three tests described in Materials and Methods section. Agarose gel electrophoresis result for each case, denoted as G0#A and G0#B, is shown in this figure.

eggs, 2 cases (2%) were found to be positive for all tests (G0#A and G0#B in Figure 2.4), which means in the genome of these two candidates, at least one copy of the vector was correctly knocked in into one *Dsx1* allele while the opposite allele harbored no insertion. Two transgenic lines namely Line A and Line B were established from the two founders G0#A and G0#B respectively.

Next, to determine the exact genotype of Line A and Line B, qPCR and sequencing were used. Result of qPCR using L32 as the reference gene indicated that in the genome of Line A one copy of donor vector existed while in Line B the copy number was two (data not shown). For sequencing results: 1) In Line A, the left junction contained a (-1;+13) mutation and the TALEN target site contained a (-6;+0) mutation. Sequence of the right junction was not determined. 2) In Line B, two copies of the donor vector were found to get tandemly integrated into the

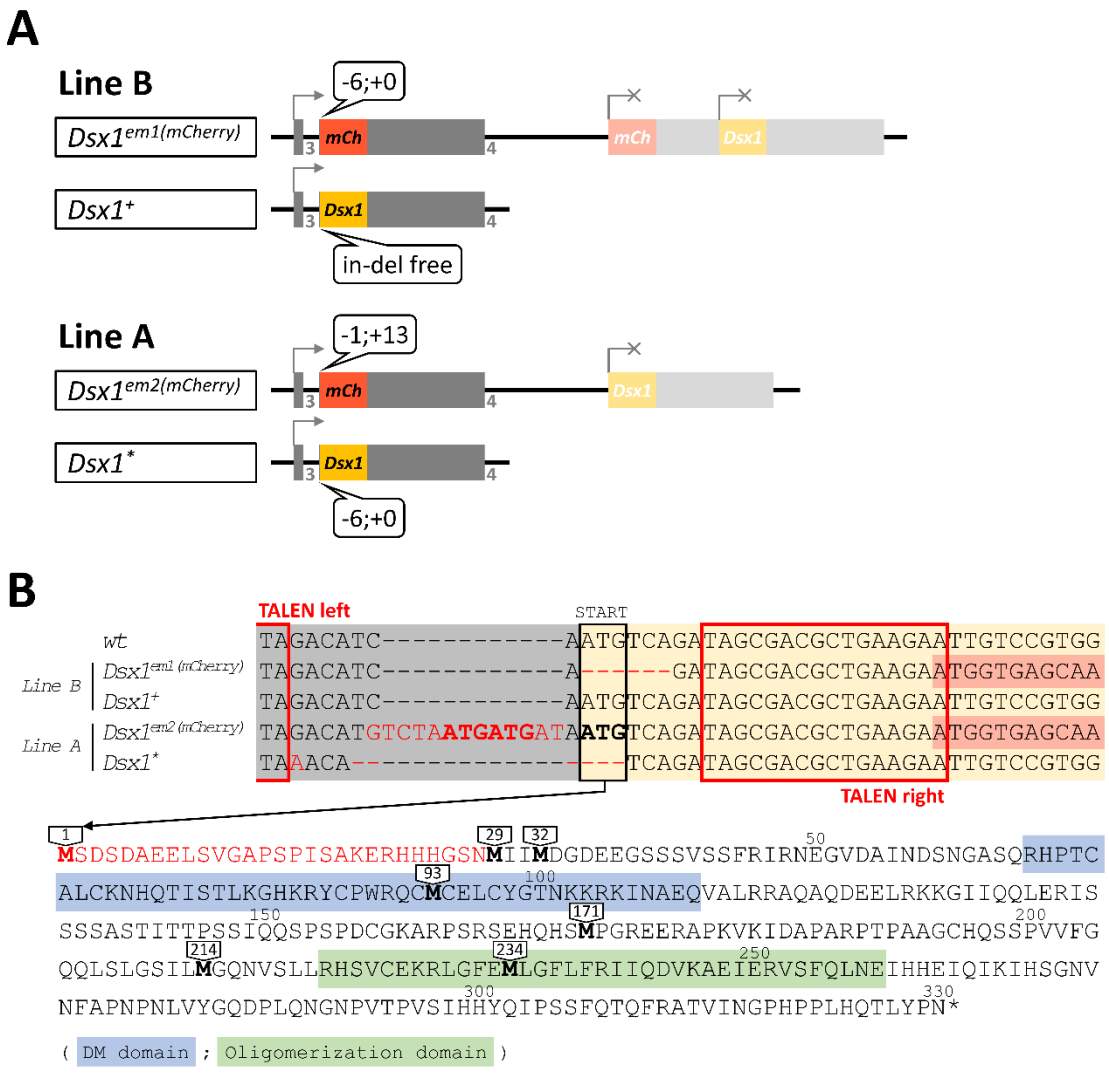

Figure 2.5: Genotype of the two *Dsx1* mutants, Line A and Line B. (A) Diagram illustrating the genotype at *Dsx1* locus of the two mutant strains, Line A and Line B. Both are hemizygous knock-ins with in-del mutations found at TALEN cleavage site. **(B)** Nucleotide sequence of in-del mutations from the four alleles shown in panel (A). At the bottom, the full amino acid sequence of *Dsx1* protein is shown together with the position of in-frame methionines that may become the alternative start codon in case the original one is deleted.

same position on one *Dsx1* locus. While the left junction and the vector connecting junction had minor in-del mutations of (-6;+0) and (-4;+16) respectively, the right junction had a large deletion of (-3748;+9). The TALEN target site on the non-inserted allele was totally mutation-free (Figure 2.5).

Because the in-del mutation on the TALEN target region in Line A eliminated the start codon of *Dsx1* ORF, unusual translation of this gene might occur. To the downstream, several alternative start codons that still preserve the protein's functional domains (both DM-domain and oligomerization domain) could be found, making it difficult to predict the impact of the mutated allele on sexual phenotype. Therefore, it would be problematic to use this mutant as a reporter strain. On the other hand, genotype of Line B was desirable with one allele still remained intact. Incorporation of a second copy of the donor vector was unexpected. However because there was no promoter that would possibly govern the expression *mCherry* in this extra copy, it should be a silent fragment. Therefore, only Line B and not Line A was chosen for validation as a *Dsx1* reporter.

2.3.4 Validation of Line B as a *Dsx1* reporter: *Dsx1* and *mCherry* male specific expression

By observing adult daphniids, I confirmed that the mCherry fluorescence was male-specific with no particular signal observed in the females (Figure 2.6A). The first pair of antennae and thoracic legs showed particularly high intensity of mCherry, similar to that previously reported for *Dsx1* [80]. mRNA level of *Dsx1* and *mCherry* in young embryos of Line B was also measured using qPCR and as a result, the male-biased expression could also be verified for both genes (Figure 2.6B). However, from qPCR data, I noted that *Dsx1* level in Line B male is just roughly half of that in wildtype male, probably because of the lack of one *Dsx1* copy in Line B genome. Nevertheless, these results indicated that the knock-in *mCherry* reporter could faithfully recapitulate *Dsx1* expression pattern.

2.3.5 Validation of Line B as a *Dsx1* reporter: male morphology and reproductive function

Because the genome of Line B has one less copy of *Dsx1* compared to wildtype, I expected that certain adverse effects toward the animal's physiology might take place. To confirm, I observed the morphology of several dimorphic characteristics using adult daphniids (Figure 2.7). I found that both male and female of this mutant exhibited typical phenotypes. Males were smaller in size,

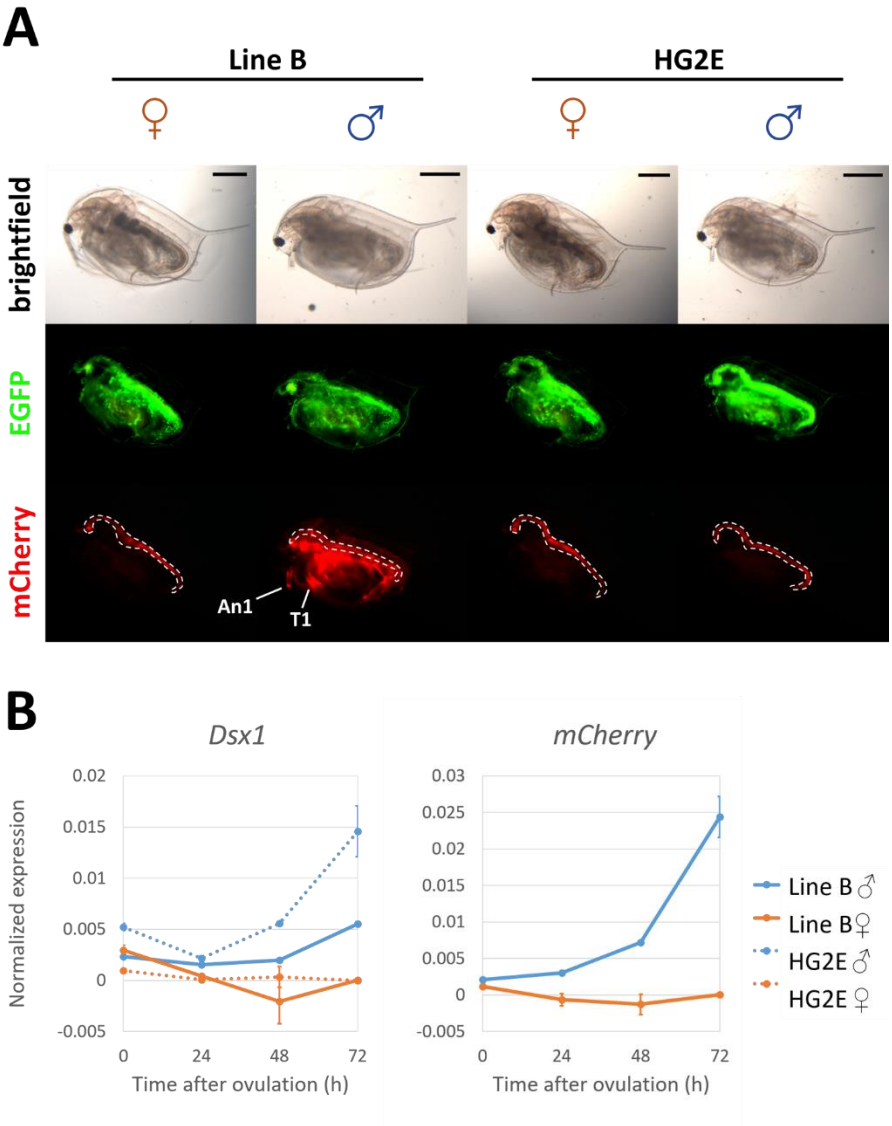

Figure 2.6: Male-specific activity of *mCherry* in Line B. (A) Nine-day-old fully matured daphniids were observed. Ubiquitous green fluorescence is caused by the EF1α-1::h2b-gfp background genotype. In all cases, the red signal from the guts (dotted lines) represents the autofluorescence of *Chlorella*, the main food used in daphniid culture. An1: first antennae. T1: first thoracic legs. Scale bars = 0.5 mm. **(B)** Embryos of 0, 24, 48 and 72 hours post-ovulation were collected for quantification of *Dsx1* and *mCherry* mRNA level. Normalization was done using L32 (a ribosomal protein encoding gene) expression. N = 3. Error bars indicate SEM.

with an angular rostrum and a prolonged first pair of antennae, a curve-opened carapace, and a pointed penis. Females had a bulky rostrum with reduced antennae, the genitals were rounded, and the carapace edge was less exposing.

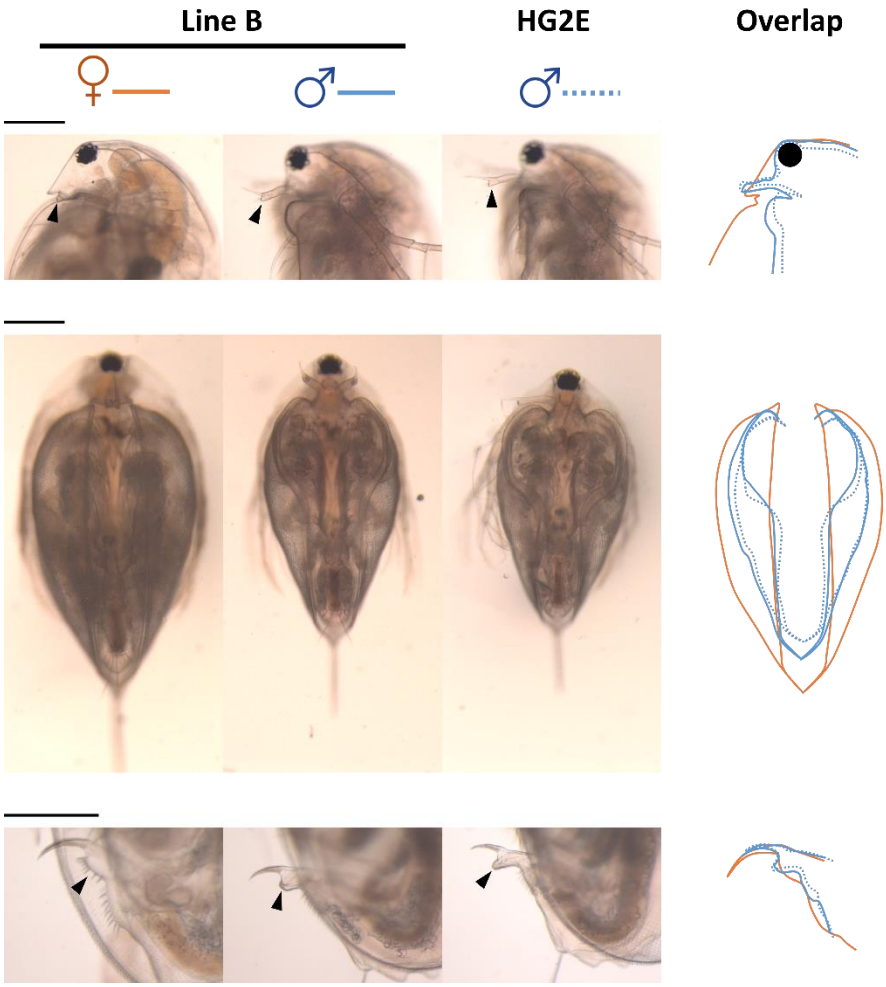

Figure 2.7: Dimorphic morphology of Line B. Adult (21-day-old) male and female of Line B showed typical morphology. From top to bottom: side view of the anterior region showing the rostrum and first pair of antennae, full body ventral view showing the edge of the large carapace, and side view of the posterior region showing the genital. For comparison, the morphology of males from the background strain HG2E is included. Black arrow head: first antenna. White arrow head: genitalia. Tracing lines on the 'overlap' panels depict the outline of each body structure of interest. Scale bars = 0.5 mm.

However, when these sex-specific traits were overlapped with wildtype of the same age for a closer comparison, minor feminization effect was detected. In detail, the first antennae of Line B males were thicker and slightly shorter than those of the wild-type ones. Their body length was also considerably larger, with the edge of the carapace curved into a less angular shape. Particularly, their penises could not achieve the typical acute outline and instead appeared rather

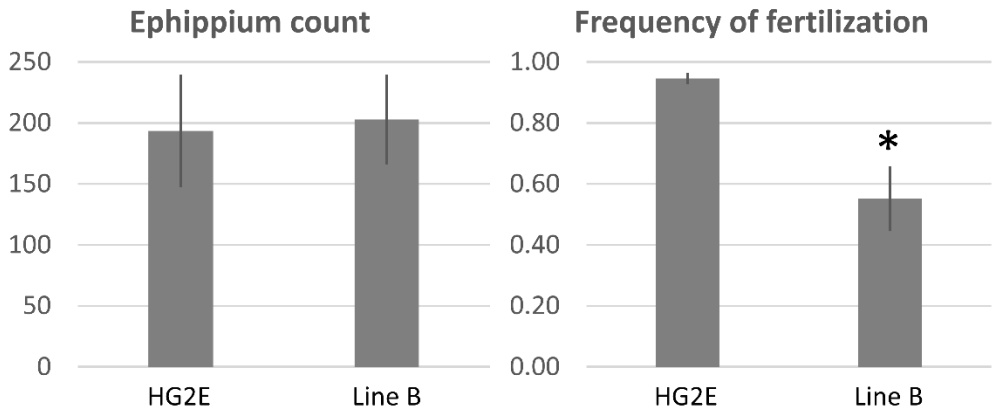

Figure 2.8: Reproductive function of Line B male and female. In this reproduction test, daphniid populations were subjected to stressful conditions to induce sexual reproduction. For each strain (Line B and HG2E), 175 females and 25 males were cultured as one population with triplicate for 4 weeks and ephippia were collected at the end of cultivation. Total ephippia were counted and the frequency of fertilization was calculated (see Materials and Methods) separately for each population. Graphs show mean values from the triplicates. Error bars indicate standard deviation. *$p < 0.05$ (t-test).

blunt. In other words, the morphology of Line B male was different from wild-type male in which there was a slight shift towards a feminine appearance.

Following the morphology observation, a reproduction test involving the crossing between male and female of Line B was performed. Ephippia and resting eggs was successfully obtained, indicating that females could produce sexual eggs and males could mate and fertilize normally (Figure 2.8). The efficiency of females creating ephippia was comparable between Line B and wildtype, suggesting that their ability to enter sexual reproduction mode in response to stressful conditions was unaffected. However, the frequency of successfully fertilized eggs was reduced by 1.7-fold, implying that there was a reduction in reproductive function of Line B males.

Despite the minor feminization observed in Line B male, there seemed to be no severe effect on the animal's fitness. Together with the result of *mCherry* male-specific expression, I could validate that Line B can be used as a reporter strain for *Dsx1* activity.

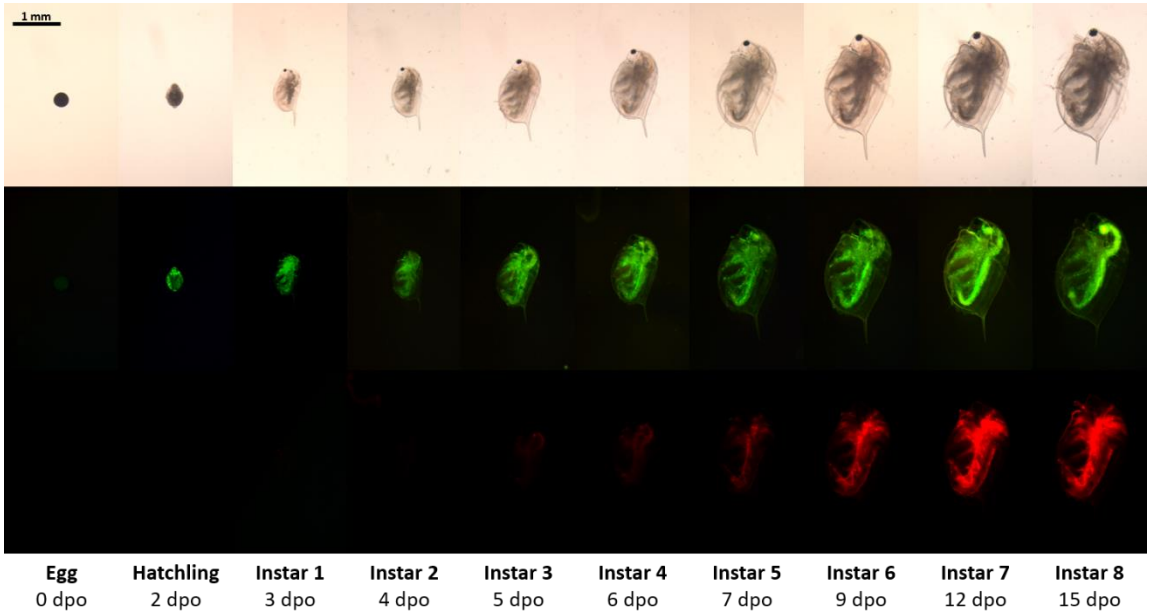

Figure 2.9: Temporal change of mCherry fluorescence in Line B male. Pictures of Line B male from different development stages were recorded. The first swimming juvenile released from the mother's brood chamber (usually 3 days after ovulation) is designated as instar 1. Every time the animal moults, it moves to the next instar stage. Typically, after 4–6 moults, daphniids become matured adults. Pictures were taken using the same camera settings. dpo: day(s) post-ovulation.

2.3.6 Mapping *Dsx1* expression using Line B: juvenile and adult

After proving that *Dsx1* expression could be visualized using Line B, a record of mCherry fluorescence were created so that it can be use as map of *Dsx1*-active, or in other words masculinized, tissues.

First, mCherry photos were periodically captured each time the animal molted. Throughout development, as the animal gradually matured, GFP intensity remained stable while mCherry intensity increased steadily (Figure 2.9). In the early stages, red fluorescence was weak and restricted to certain locations. With maturation, fluorescence intensity increased and expanded to a wider range of tissues.

Next, mCherry expression was observed closer using Line B male embryos at 14-, 24-, 42-h post-ovulation (hpo), juveniles at 72 hpo and 6 days post-ovulation (dpo), and adults at 14 dpo (Figure 2.10). Based on my observation,

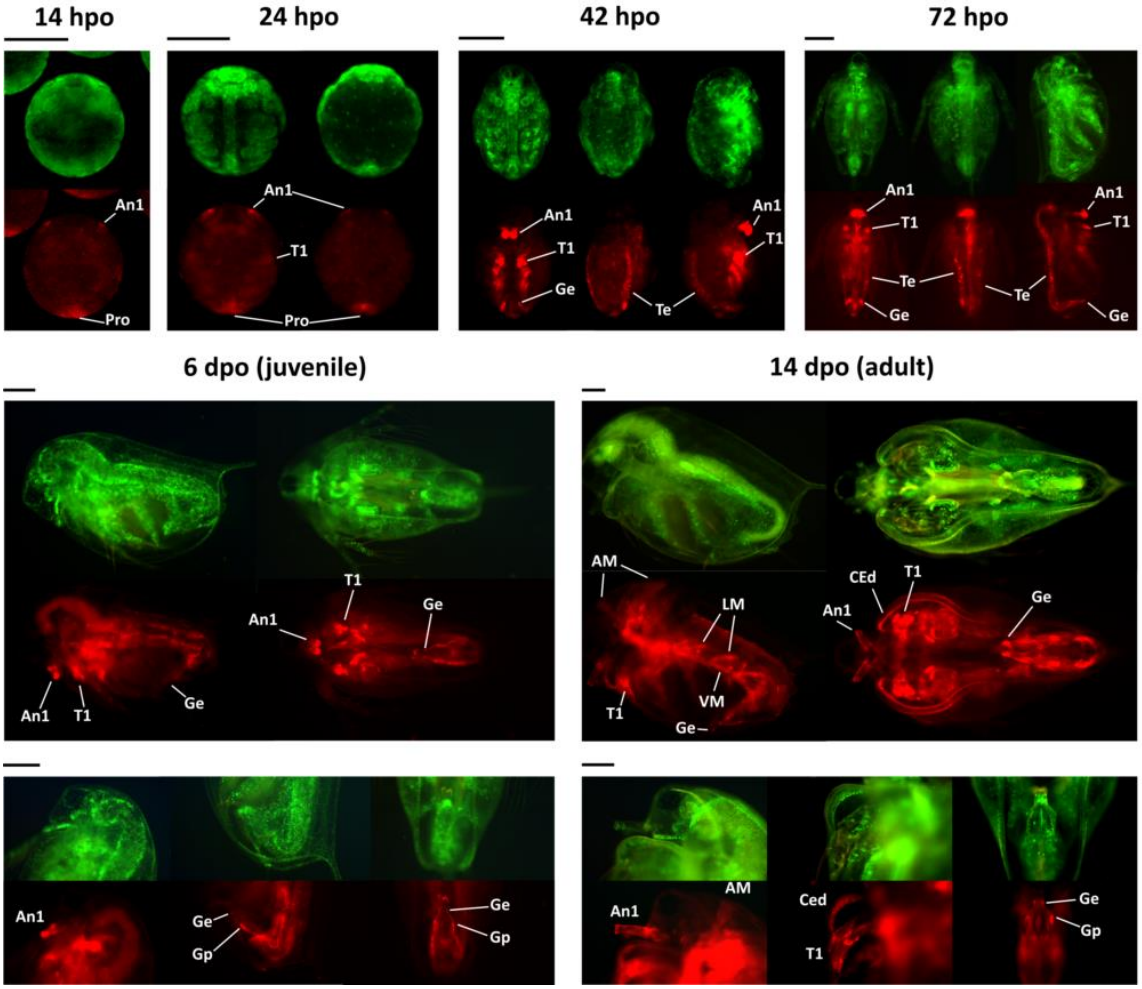

Figure 2.10: Spatially and temporally specific expression of mCherry in Line B male. All embryos and daphniids shown in this figure are males of Line B. hpo: hours post-ovulation. dpo: days post-ovulation. For the 14 hpo panel: ventral view. For the 24 hpo panel: ventral view (left) and dorsal view (right). For the 42 hpo and 72 hpo panels: ventral view (left), dorsal view (middle), and side view with the ventral side facing right (right). A1: first antenna, T1: first thoracic leg, Pro: proctodeum, Ge: genital (i.e. penis in this case), Te: testis, AM: antennal muscle, LM: lateral muscle, VM: ventral muscle, CEd: carapace edge, Gp: gonopore. Scale bars = 200 μm.

major developmental stages corresponding to the presence of mCherry in male animals can be described as follows:

(i) Right before body segmentation occurred (14 hpo), the mCherry signal was obvious in (1) the rudiment first pair of antennae and (2) the posterior zone around the proctodeum. At 24 hpo, embryos started to exhibit strong mCherry

fluorescence in the pair of first thoracic legs as well as weaker signal in the other thoracic segments.

(ii) In later embryos (42 hpo), mCherry signal was primarily found in (1) the pair of first antennae, (2) pairs of thoracic legs, and (3) testes and spermiduct-genitalia system. At 72 hpo, among the thoracic legs, intense signal was maintained only in the first pair.

(iii) Following the onset of maturation, the signal in the testes gradually weakened and seemed to disappear at 6 dpo. On the contrary, a collection of other male-specific structures began to strongly express mCherry. In adult males (14 dpo), the signal was particularly intense in (1) the pair of first antennae, (2) the pair of first thoracic legs (which had already developed into copulation hooks), (3) the carapace edges below the helmet, (4) the skeletal muscle system, and (5) penises and gonopores.

Interestingly, the timing of *mCherry/Dsx1* activation in male-specific structures corresponded to the tissue's masculinization level. Until instar 4 (6 dpo), except for the elongated first antennae and the gonad, there was no clear dimorphism between males and females (Figure 2.9, until Instar 4). From instar 5, a surge in *Dsx1* activity occurred, as shown by the rapid accumulation of mCherry into several male-specific structures including the carapace edge below the helmet, the tip of the penis, and the skeletal muscle (Figure 5, from Instar 5 and Figure 2.10, 14 dpo). Clear transformation of the young juveniles into matured males was observed, in which the carapace edge began to curve at the mCherry-expressing section to create an opening and the tip of the penis was raised to form an acute shape. These results suggest that there is a time- and site-specific role of *Dsx1* in which this gene is recruited only when and where it is needed, and once activated, it begins to dictate the masculinization of that tissue.

2.3.7 Mapping *Dsx1* expression using Line B: embryogenesis

To understand which cell population first shows *Dsx1* expression, a time-lapse observation of the early stages of development was performed using Line

B male embryos. By observing the H2B-GFP signal, I could distinguish six different early embryonic stages: (i) gastrulation, (ii) mesendoderm expansion, (iii) stomodeal invagination, (iv) cumulus migration, (v) naupliar segmentation, and (vi) postnaupliar segmentation (see [99] for a description of *Daphnia magna* embryonic stages, also I could identified two previously undescribed stages, (iii) and (iv)). At 11 hpo, a second gastrulation, termed stomodeal invagination, occurred between the blastopore and the anterior end, forming the origin of the mouth. From 11 to 16 hpo, the internalized cells, named “cumulus”, migrated along a midline, situated on the ventral region, towards the caudal side (Figure 2.11).

Although no particular signal was detected until stage (ii), I found that mCherry was first localized at the cell cumulus that appeared around the site of stomodeal invagination. At the same time, a second signal could also be found around the blastopore. As development proceeded, together with the cumulus, the mCherry-expressing cell cluster migrated towards the blastopore and gradually became less localized. In parallel, the second mCherry-expressing cell cluster moved downwards until reaching the posterior. It was not clear whether those two mCherry-expressing cell clusters merged, but the closer they got to the posterior region, the stronger the red fluorescence became. At stage (v), as the buds of the first antennae emerged, the mCherry signal also intensified in this region. Along the border of the head and body segments, a significant signal was also detected. At stage (vi), thoracic segmentation began, and the five segments appeared in order from anterior to posterior. The first segment, which would later develop into the male-specific copulation hook in adults, strongly expressed mCherry. Fluorescence was also detected in other segments, but at a lower level. Just before hatching, embryonic regions exhibiting mCherry were: (1) around the proctodeum, (2) the first antennae, (3) thoracic segments especially the first one, and (4) the head-body border (Figure 2.11).

The same observation was also performed for Line B females. Very similar mCherry patterns were observed prior to segmentation. mCherry signal was detected in the migrating cumulus and blastopore/proctodeum area, but it was

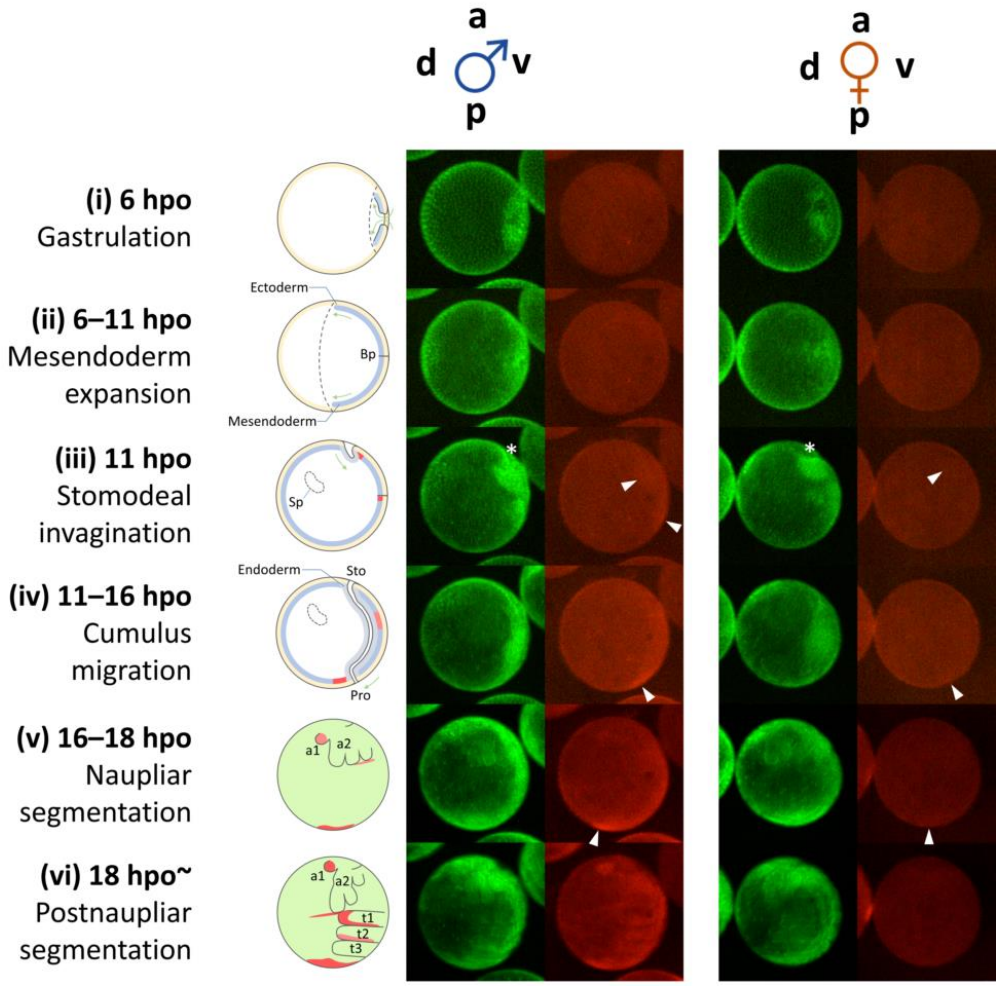

Figure 2.11: Dynamic progression of *Dsx1*-expressing cells during early embryogenesis. This snapshot series of a males and a female embryo of Line B was extracted from my time-lapse observation, showing major events from gastrulation until thoracic segmentation. Schematic diagrams on the right illustrate simple anatomy of the embryos at the corresponding time points. The diagrams from stage (i) to (iv) show images of embryonic sections. The diagrams (v) and (vi) show superficial views of embryos. a: anterior, p: posterior, v- ventral, d: dorsal, Bp: blastopore, Sp: Scheitelplatten, Sto: stomodeum, Pro: proctodeum, t1–3: thoracic segments, a1: first antenna, a2: second antenna, hpo: hours post ovulation. White arrow heads indicate mCherry-expressing cell clusters that migrate in an anterior-to-posterior direction. An asterisk at stage (iii) indicates the site of invagination.

much weaker comparing to that observed in Line B males. From stage (v), the signal neither intensified nor appeared elsewhere in females. These results were consistent with previously obtained data using qPCR, except for the expression

patterns at 6 hpo when *Dsx1* was expressed in both male and female embryos [81,100]. This contradiction probably resulted from the rather weak expression level of the *mCherry* reporter, which might be indistinguishable from the noise generated by the yolk protein.

2.4 Discussion

In this chapter, by using a TALEN-mediated gene editing approach, I could successfully generated a transgenic strain of *D. magna* that allows visualization of *Dsx1* expression with mCherry fluorescence. This *Dsx1* reporter strain, named as Line B, highlights the strict temporal and spatial synchronization of *Dsx1* expression and the development of sexually dimorphic traits. Two features of *Dsx1* expression patterns will be discussed.

First, *Dsx1* expression is spatiotemporally regulated and maintained in male-specific traits. This feature is consistent with the DM-domain genes found in other studied organisms such as fruit fly [101–104] and mouse [105,106]. In mammals, *Dmrt1* (a mammalian DM-domain gene) is upregulated during late testicular development, and its expression in the testis is consistently maintained by a positive regulation loop involving *Sox9*, *Fgf9*, and *Ptgdr* until adulthood [107]. In *Drosophila*, in addition to sex-specific splicing, *dsx* is regulated at the transcriptional level and exhibits ongoing expression for the maintenance of sexual traits in a small subset of cells located in the dimorphic tissues [103,108]. Therefore, my data supports a common idea: sex-determination is restricted temporally and spatially in the ability to recruit a DM-domain gene. This DM-domain gene serves as a binary switch and once it is activated, this gene subsequently takes over the role of sex maintenance. It also means that a vast proportion of cells in the body are neither male nor female, or in other words, sexually neutral.

Second, male-specific *Dsx1* expression begins in a specific cell cluster of early embryos. The specific cell population “cumulus” first expresses mCherry at the stomodeal invagination stage, and it subsequently migrates towards ventral regions, from rostral to caudal, along a midline. The functions of similar migrating

cell populations have already been characterized in other animals. In chicken, a mass of cells called “Hensen’s Node” shows similar movements during gastrulation and neurulation [109]. In spider, a cell mass named “cumulus” has also been reported to appear at the central blastopore and migrate centrifugally [110]. Importantly, both migrating cell masses function as primary organizers and secrete common molecules such as BMP/Dpp for axial pattern formation [111]. This suggests that the primary organizer is sexually plastic in *D. magna*, meaning that this cell cluster is sexually bipotential and can differentiate into male or female form, which in turn induce sex differentiation of neighboring tissues accordingly. Following migration, the cumulus was located and started to show stronger fluorescence in the posterior region, or posterior growth zone. Posterior growth and segmentation are known to be accomplished by the supply of progenitor cells from the back end of the embryo [112]. I speculate that *Dsx1*-expressing progenitor cells would be distributed from the posterior growth zone in early embryos across the body during axial elongation. Considering the phylogenetic position of the cladoceran crustacean *Daphnia* [40,41], this behavior might be a conserved feature of the DM-domain gene in this clade. However to my knowledge, this is the first time-lapse imaging-based tracking of DM-domain gene expression in early embryos, further comparative expression analyses in other organisms will be necessary to determine the similarity of DM-domain gene expression in early embryos.

CHAPTER 3: WHOLE BODY TRANSCRIPTOMIC PROFILING REVEALED A NETWORK OF NON-BINARY GENES UNDERLYING INTERSEXUALITY

3.1 Introduction

The *Dsx1* gene of *D. magna* was previously identified as a sex determining factor using the reverse genetic approach, in which this gene was originally chosen because of the highly conserved sequence and function of the DM-domain gene family [80]. Locating other genes revolving around *Dsx1* might not be as simple because upstream sex determining and downstream sex differential genes tend to become more diverse the farther they are from the core factor [27]. To have a good prediction of gene candidates, aside from referring to other species, transcriptomic characterization of the species of interest is arguably the most popular approach in recent years. For *Daphnia*, although male and female transcriptomes have already been published [113–116], there is still a gap of information, as: 1) Available transcriptomes only focus on adult male. According to previous data as well as my observations in Chapter 2, *Dsx1* expression undergoes several phases during daphniid maturation, indicating that the composition of *Dsx1* cascade might not be the same at every stage. It would be necessary to obtained more diverse data in term of stage of development. 2) Of the thousands sex-biased gene detected, it is difficult to predict which gene is upstream, downstream or perhaps unrelated to *Dsx1*. In order to have a hint, a method that is usually applied is to alter the activity of the gene of interest, for example by knock-down or overexpression, and see how the transcriptome is shifted.

Line A obtained in Chapter 2 became the tool that can be used to solve both problems. In Line A, not only one *Dsx1* copy was knocked out due to integration of the reporter plasmid, the remaining copy also harbored a 6-bp deletion that eliminated *Dsx1* start codon. This genotype led to severe feminization in males of Line A, as will be described later, but was neutral to

females, resulted in a special *Daphnia* strain from which intersex daphniids can be produced readily. This allows the generation of intersex transcriptomes at will without worrying about limitation of sample source, which usually is impossible because intersex animals are extremely rare and generally sterile. In this chapter, I describe about the intersex phenotype of Line A as well as the information obtained from analyzing their transcriptomes.

3.2 Materials and Methods

3.2.1 *Daphnia* culturing and male production

Daphnia NIES strain, HG2E strain together with Line A and Line B were maintained in asexual cycle using the optimal culturing condition described in Chapter 2 (Section 2.2.1). Noted that the fed *Chlorella* amount was increased to 1.28×10^9 cells due to a change of provider. For fluorescence photographing, I fed 0.3 mg dry yeast for one daphniid daily instead of algae to avoid the autofluorescence usually found in the gut.

Production of male daphniids including the intersex 'males' of Line A and Line B was done using the Fenoxycarb exposure method as described in Chapter 2 (Section 2.2.10).

3.2.2 Crossing of *Daphnia* strains

Crossing between strains requires sexual reproduction, which is inducible by putting the population under high density and starvation as already described in Chapter 2 (Section 2.2.10). Specifically in this chapter, I mixed 25 young males of Line B with 175 young females of Line A in one beaker containing 1 L ADaM and fed with 4.8×10^8 *Chlorella* cells daily (again, this increase in feeding amount was due to a change of provider). Ephippia were harvested after 3 weeks of culturing and stored in dark at 4°C for one year.

To trigger the hatching, the ephippia were first air-dried overnight at room temperature, followed by rehydration in ADaM for 2 hours [117]. All ephippia were then opened to retrieve the resting eggs inside [118]. I incubated these activated

resting eggs at standard culturing condition for one week and collected all hatched juveniles for genotyping. Genotyping method was the same as screening for mutants described in Chapter 2 (Section 2.2.8).

3.2.3 Sampling of daphniids and RNA extraction

For samples that were not used in RNA-seq experiments, 20–30 embryos of the same clutch or 2–3 adults of the same age were collected as one sample with triplicate for each group. For samples used in RNA-seq, because a larger amount of RNA was needed, I pooled 40 h embryos from three mothers as one sample, also with triplicate for each group. As it was difficult to find mothers that lay eggs at the same time, immediately after oviposition, those releasing eggs earlier were kept in 4°C to wait for the others. This short-term ice-chilled preservation can efficiently suppressed biological processes such as hardening of egg shell and cytokinesis for up to two hours without damaging the *D. magna* eggs [85]. Once all ovulated mothers were obtained (typically in less than one hour for each group), the daphniids were returned to normal condition and cultured for 40 hour before subjected to dissection and isolation of embryos. Using this method, I could ensure that all embryos in one sample were perfectly synchronized at the time of sampling.

Immediately after collecting, all samples were transferred to liquid nitrogen for flash-freezing. RNA extraction was performed shortly after by using Sepasol-RNA I solution (Nacalai Tesque, Kyoto, Japan), followed by phenol-chloroform purification and DNase treatment to remove genomic DNA contaminant.

3.2.4 qRT-PCR

Total RNA was subjected to cDNA synthesis using random hexamers (Invitrogen) and SuperScript III Reverse Transcriptase (Invitrogen). For qPCR, PowerSYBR® Green PCR Master Mix (Invitrogen) was used and reactions were carried out inside an Mx3005 P Real-Time PCR System (Agilent Technologies, CA, USA). The ribosomal protein L32 gene, whose whole body expression level was proven to be highly stable during development [119], was used for

normalization of all other genes. Sequences of all qPCR primers can be found in Table S1.

3.2.5 RNA sequencing

I used the mRNA-seq service provided by Novogene (jp.novogene.com). According to the company, the submitted total RNA samples were first eluted through oligo(dT) columns to enrich mRNA. Then cDNA was synthesized using random hexamers followed by terminal repair and sequencing adaptor ligation to generate cDNA libraries. All 12 libraries passed their QC and were fed into Illumina sequencers for paired-end sequencing. Raw data filtering and adapter trimming were done as part of the service. What I received were clean data of ~10,000,000 read pairs per library and read length was 150 bp.

3.2.6 RNA-seq data analysis

All analyses were done using the CLC Genomics Workbench software (Qiagen). Details about parameters that were used are as follows: 1) Mapping: mismatch cost = 2, insertion cost = 3, deletion cost = 3, length fraction = 0.8, similarity fraction = 0.8, global alignment = no, auto-detect paired distances = yes, strand specific = both, maximum number of hits for a read = 10, count paired reads as two = no, expression value = total counts, calculate expression for genes without transcripts = no, 2) Differential expression analysis (Empirical analysis of Digital Gene Expression (EDGE) test): total count filter cutoff = 5.0, estimate tagwise dispersions = yes, exact test comparisons = all pairs, 3) Heat map clustering: distance measure = Euclidean distance, cluster linkage = average linkage, filter settings = specify features, 4) K-medoids clustering: number of clusters = 24, distance metric = Euclidean distance, data level = group means, data to cluster = normalized expression values, subtract mean gene expression level = yes, 5) Annotation test (hypergeometric test): annotation to test = GO biological process, reduce feature set = no, values to analyze = normalized expression values, full set = D. magna 47,109 gene set, subset = female-biased or male-biased gene set. Assignment of GO terms to each gene was carried out using Blast2GO (BioBam). For mapping, I used the 2010 D. magna genome

assembly v2.4 (GenBank accession LRGB00000000) together with the 2014 D. magna evg7f9b gene set as reference [71]. This gene set contains 29121 gene loci together with 17228 “culled” transcripts which may as well contain some valid loci. Among these genes, some are split-mapped, meaning that they consist of two fragments that mapped to distant positions in the genome assembly. Because these split-mapped genes disturb the visualization of gene distribution on the genome by the CLC Genomics Workbench software, I edited the gene set and treated the split fragments as two different genes. As a result, there are total 47,109 genes in the full set of my analysis. Also, although the original ID of each gene is in the format [Dapma7bEVm][6 digits], I added 7 characters indicating the scaffold/contig the gene is mapped to and 7 characters indicating its split attribute to make new unique IDs. Please refer to my deposited data (see section 3.5, Data availability) for detailed expression profile.

3.2.7 Statistical analysis

Processing of qPCR data was done using Microsoft Excel 2016. Mean values were obtained using the “average” function. SEM (standard error of the mean) values were obtained by dividing the standard deviation (obtained using the “stdev” function) by the square root of number of samples. For pair-wise statistical comparison, first an F-test was done by using the “f.test” function (only p-value will be calculated) to determine whether the variance of the two groups are equal or unequal. Since most pairs showed unequal variance (p-value threshold of 0.05), one-tail t-tests for two sample with equal variance were performed for all pairs by using the “t.test” function (only p-value will be calculated). Charts are generated also by using Excel in combination with PowerPoint.

3.3 Results

3.3.1 Intersex phenotype of Line A male and Line B male

As mentioned in Chapter 2 (Section 2.3.5), Line B males exhibited minor feminization at non-gonadal tissues in which little shift in morphology of male specific structures toward female appearance was detected. Although reduction

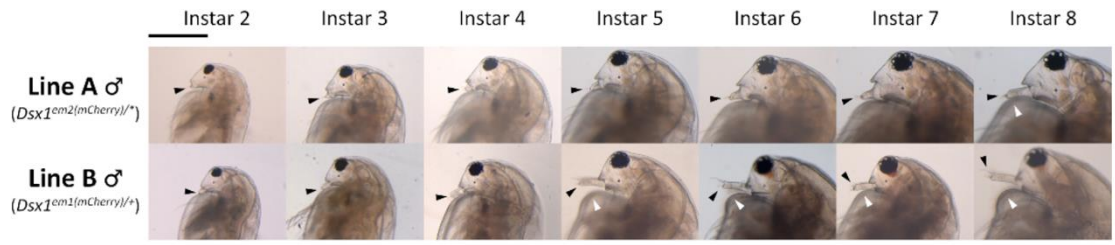

Figure 3.1: Head region with focus on the first pair of antennae of Line A males and Line B males of various ages. Until instar 4 is the juvenile stage of daphniids. Transition to fully mature adults usually occurs when the animal reaches instar 5, which is approximately one week after birth. Black-arrow heads: first antennae. White arrowheads: carapace curve that reveals copulation hooks in males. Scale bar indicates 0.5 mm.

in mating ability was also found, Line B males could still successfully fertilize and create viable resting eggs.

I continued to examine the effect of Line A genotype on sexual differentiation by observing phenotype of males that were produce by Fenoxycarb exposure. In Line A, severe feminization took place from a very early stage of development and persisted until adulthood. In particular, the first pair of antennae of Line A male was obviously elongated which is a distinctive trait of male daphniids. However the length was short comparing to Line B male or wildtype male. This difference was visible in juveniles (instar 2–4) and became even more profound after puberty (from instar 4 to instar 5) when Line B male quickly transformed to adult morphology but Line A male showed very little change (Figure 3.1). At adulthood, feminization effect was even more obvious in many morphology aspects. In details, Line A male had average body length comparable to wildtype female, which is roughly 25% larger than normal male (Figure 3.2A and 3.2B). The ventral opening of the carapace in Line A male did not have the revealing curve around the first body segment as typically found in male but was rather straight and closed like female (Figure 3.2B). At the rostrum region, aside from the barely elongated first antennae, helmet of Line A male also showed female-like bulky appearance but not the closely fit shape of male (Figure 3.2C).

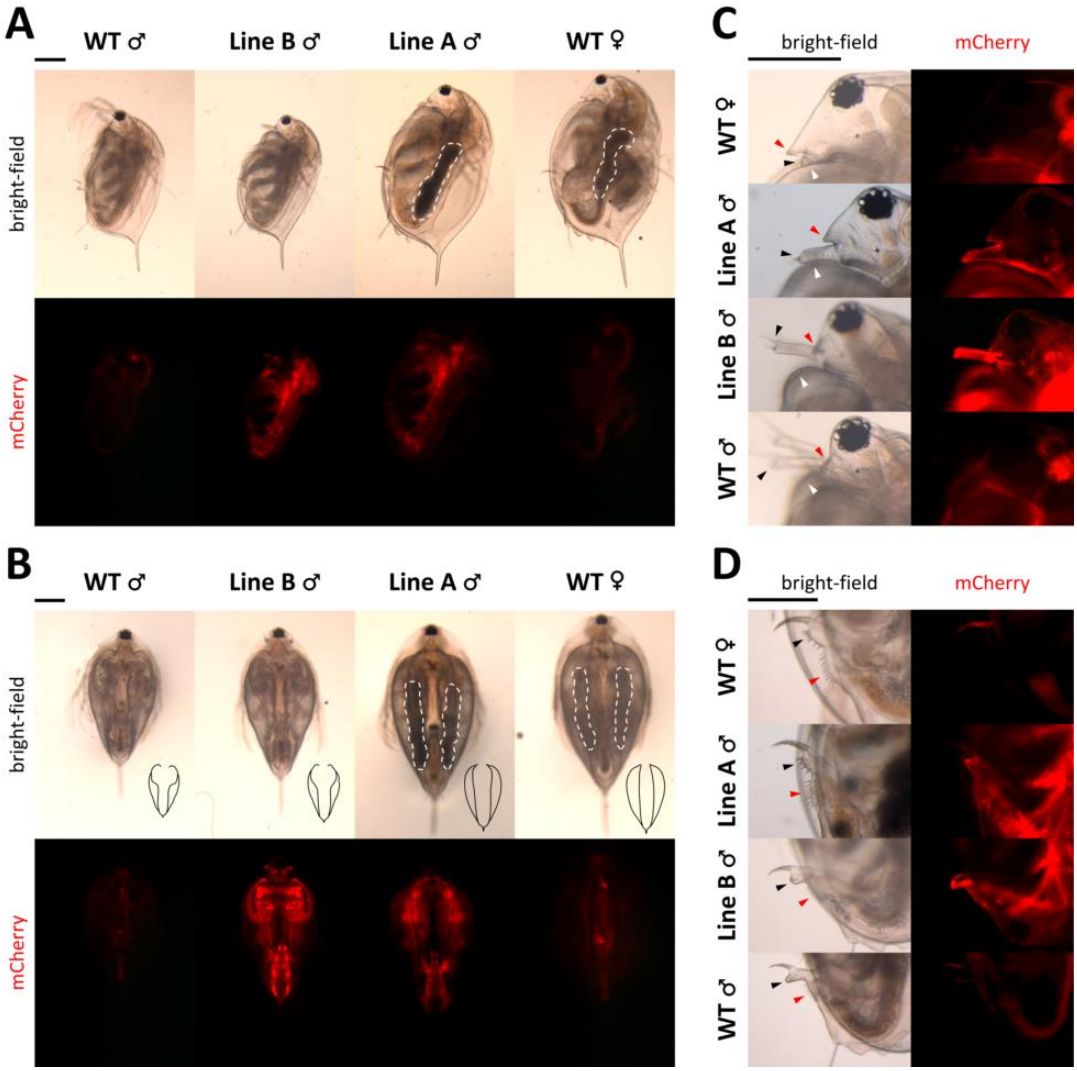

Figure 3.2: Intersex phenotypes of Line A male and Line B male. (A) Full body, side view of instar 8 daphniids. White dotted lines indicate ovary-like gonads, which appeared darker because of the accumulation of yolk protein. **(B)** Full body, ventral view of instar 8 daphniids. Black drawings at bottom right corner of each bright-field photos are tracing lines scaled down to 1:2.26 ratio depicting the outline of the carapace edge. White dotted lines have the same meaning as in panel B. **(C)** Head region, side view of instar 8 daphniids. Black-arrow heads: first antennae. White arrowheads: carapace curve. Red arrowheads: rostrum. **(D)** Genital and anal region, side view of instar 8 daphniids. Black arrowheads: genital. Red arrowheads: anus. Scale bars indicate 0.5 mm.

Furthermore, Line A male seemed to have the genital and anus resembling those of female (Figure 3.2D).

Especially, upon reaching the age of sexual maturity, irregular gonad development could be observed in Line A males. Typically, testes of male daphniids are transparent and thus impossible be recognized by naked eyes. On the other hand, ovaries of females are noticeably darkened due to the accumulation of yolk protein. In Line A male, ovary-like darkened gonads were found in all cases. However, no eggs were released from these ovary-like structures even after several weeks of culturing, making the gonads of Line A male remain thick and dark despite multiple times of molting (Figure 3.2A and 3.2B).

From this observation, I categorized males of Line A and Line B as intersexes, in which Line B male exhibited mild feminization while Line A male displayed more severe transformation to female. Assuming that *D. magna* sex is a spectrum with typical female and male occupying the two ends, Line A male and Line B male would represent two different positions in the middle of the scale.

3.3.2 Expression of *Dsx1* and *mCherry* in the mutants

As mentioned in Chapter 2 (Section 2.3.4), in Line B male, mRNA level of *Dsx1* was roughly half of that of wildtype male, possibly because of the lack of one *Dsx1* copy. To confirm the effect of mutated *Dsx1* allele in Line A on its own expression, I performed quantitative PCR using whole body samples of different ages. I found that in Line A, the dimorphic patterns of *Dsx1* and *mCherry* expression were similar to those in Line B without any statistical difference (Figure 3.3A).

Despite the same mRNA level of *mCherry*, while observing the fluorescence signal, I noticed that fluorescence intensity in the males of Line A was slightly weaker comparing to those of Line B (Line A vs. Line B, Fig 3.3B). To confirm whether this was because of the introduction of in-frame ATGs to the upstream of start codon of *mCherry* in Line A (Figure 2.5), I performed a cross using Line A females and Line B males to swap the two *mCherry* alleles. As a result, there was no difference in mCherry fluorescence between the two mutants if both had the same *mCherry* reporter sequence. I also found that the *mCherry*

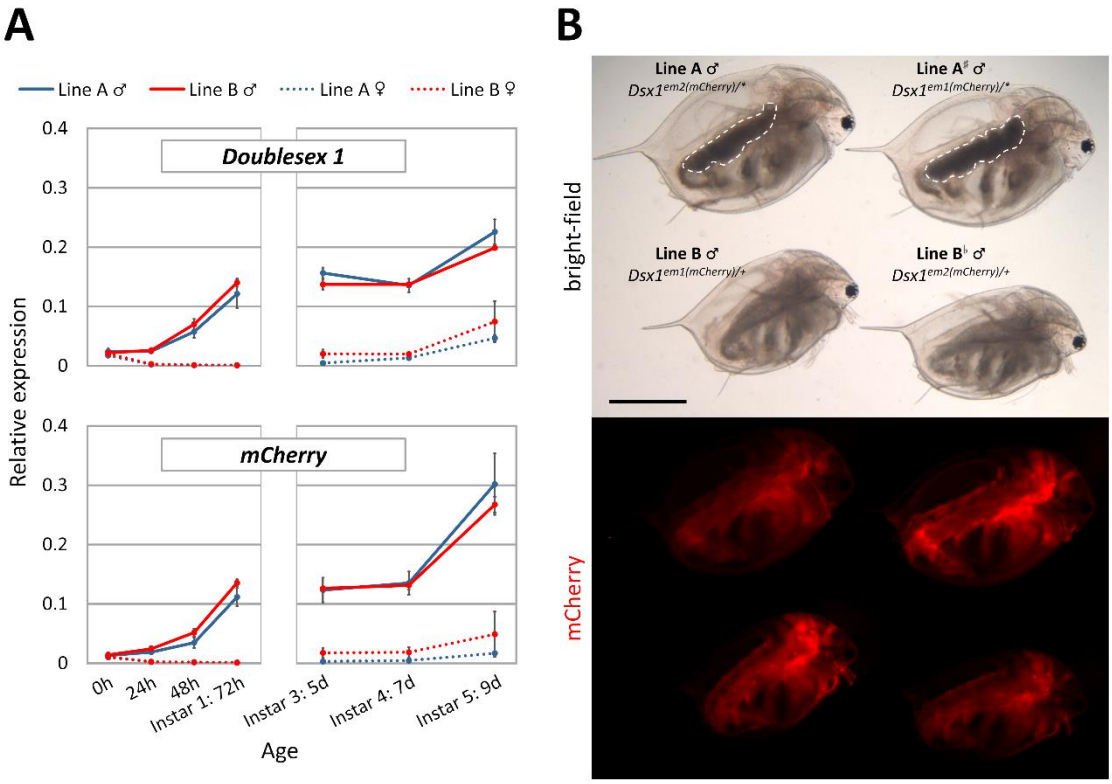

Figure 3.3: *Dsx1* and *mCherry* expression in Line A and Line B. (A) Whole body mRNA level quantified by qPCR targeting the two alleles at *Dsx1* locus. Expression of L32 gene was used for normalization. **(B)** Difference in mCherry intensity between Line A, Line B and two hybrid lines obtained from a crossing between Line A and Line B. All four daphniids are of the same age (instar 8, 17 day-old) and photographed in one single photo to allow direct comparison. White dotted lines indicate the ovary-like darkened gonads. Scale bar indicates 1.0 mm.

allele derived from Line B had better performance probably due to no upstream ATG (Line A# and Line B vs. Line A and Line Bb, Fig 3.3B).

Despite the difference in feminization level, it could be seen from these results that there was no change in transcription, translation, as well as spatiotemporal control of the Dsx1 locus (Fig 3.2, mCherry photos) between Line A male and Line B male. These data suggested that the cascade relaying male determination signal from Fenoxycarb to *Dsx1* was not disrupted by the 6-bp deletion at start codon ATG of *Dsx1* in Line A, and that only genes downstream of *Dsx1* in the pathway were affected.

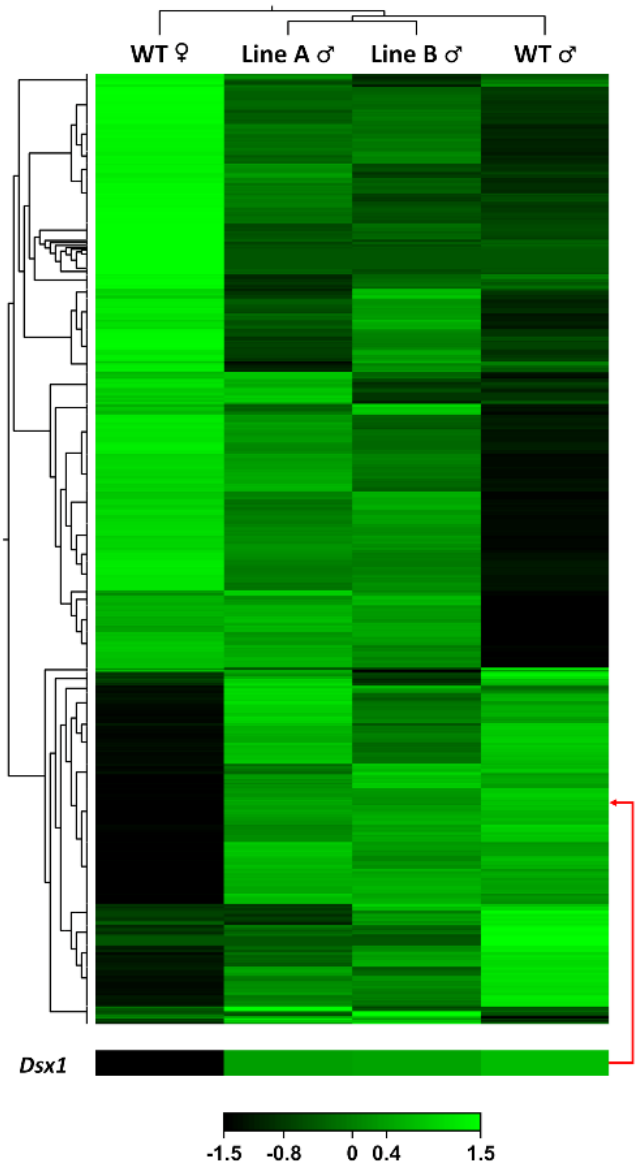

Figure 3.4: Heat map of 1354 differentially expressed genes detected in the wild type female vs. wild type male comparison. Each row represents one gene. In addition to wild type female and wild type male gene expression (left-most and right-most column), intersex gene expression is also shown (two columns in the middle). A close-in for *Dsx1* together with an arrow leading back to its original position is provided at the bottom of the heat map. Color scale indicates normalized logCPM values in which brighter green means stronger expression.

3.3.3 Non-binary global gene expression along sex spectrum in 40 h embryos

Since Dsx1 is a transcription factor, its direct and indirect target genes must have been affected transcriptionally in the mutants. Therefore, in order to characterize this shift in transcriptome of intersex animals, RNA sequencing approach was used. 40-hour embryos of wildtype female, Line A male, Line B male and wildtype male were chosen as representatives of four different positions in *D. magna* sex spectrum for this experiment. I targeted the stage of 40 hours

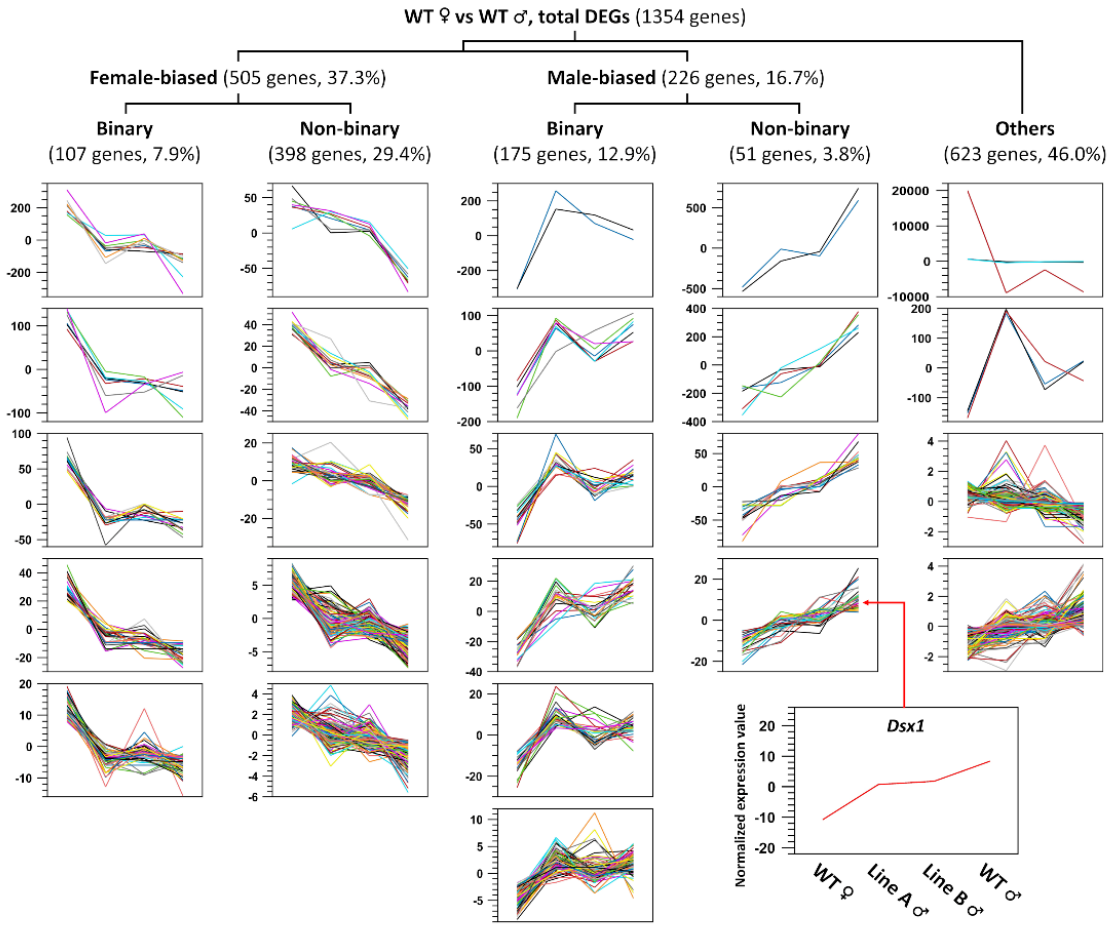

Figure 3.5: K-medoids clustering of 1354 genes showed in Figure 3.4. In contrast to the log-transformed expression value used in the heat map, normalized read count values were used in this k-medoids clustering to allow visualization in better resolution. All genes were split into 24 clusters based on their trend of expression (which was already mean-centered) across the 4 positions of sex spectrum (WT female, Line A male, Line B male, WT male). These clusters were subsequently grouped into 5 categories based on their dimorphic properties (see main text for details). *Dsx1* was identified as a non-binary male-biased gene in this analysis (bottom right graph).

post oviposition (hpo) for two main reasons. Firstly, gene expression in older daphniids may fluctuate greatly under the influence of molting cycle and environmental factors. It is much easier to obtain synchronized samples from embryos in which the *Dsx1* cascade would stand out more without noises from other gene networks. Secondly, according to the phenotyping result, morphological difference was obvious even in first swimming juvenile (72 hpo),

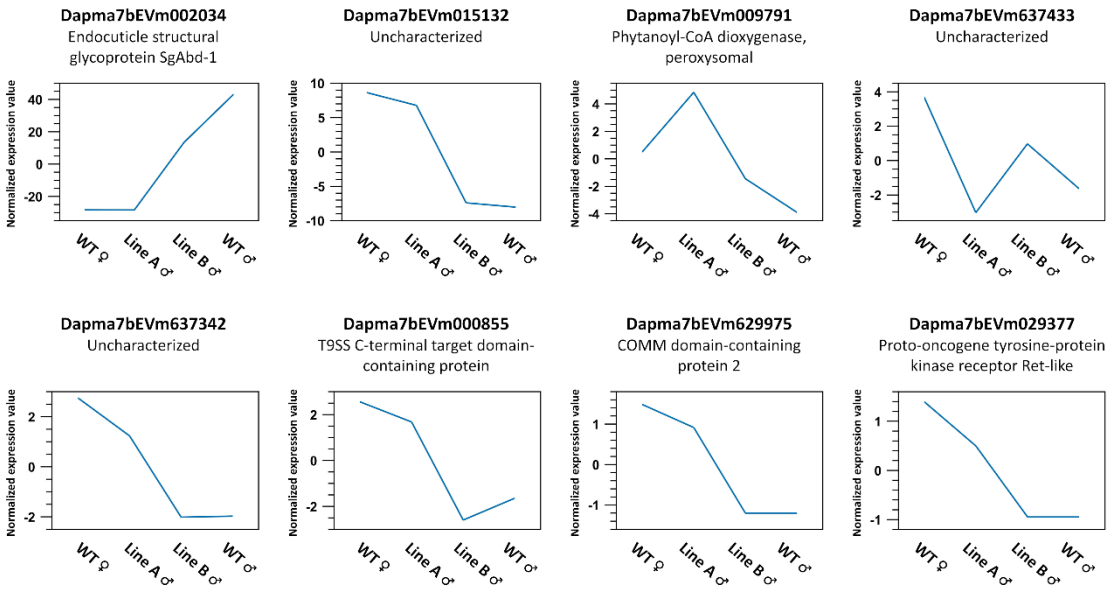

Figure 3.6: Eight genes showing differential expression between Line A male and Line B male. These genes were identified by applying a filter of p-value < 0.05, absolute fold change ≥ 1.2 (EDGE test) in Line A male vs. Line B male comparison to the list of 731 sex-biased genes. Graphs have same meaning as those from K-medoids clustering in Figure 3.5.

indicating that segregation of sex differentiation cascade had already occurred during organogenesis (16–24 hpo).

Total 12 RNA sequencing libraries were generated from triplicate of each of the four sexual phenotypes. I first focused on those that differentially expressed (DE) between wildtype male and wildtype female. With the cut-off threshold of p-value < 0.05 and absolute fold change ≥ 1.2 (Empirical analysis of Digital Gene Expression (EDGE) test), 1354 DE genes were identified and I found that *Dsx1* also belonged to this list (Figure 3.4). To further categorize these genes based on their expression profile along the sex spectrum, I performed K-medoids clustering using normalized expression values (reads per million). As a result, I found 505 genes (37.3%) showing female-biased expression and 226 genes (16.7%) were male-biased. Interestingly, among these genes, 449 (33.2%) showed non-binary expression profile, in which their activity seemed to be at intermediate level in intersex samples. These cases were referred to as non-binary genes, and the

majority of them (398 genes) belonged to female-biased group. Other genes whose expression did not seem to be affected in intersex animals and remained comparable among the male groups regardless of *Dsx1* mutation types were referred to as binary genes (282 genes). *Dsx1* was detected as a male-biased and non-binary gene in this analysis, which is consistent with previous qPCR data. I disregarded the remaining 623 genes (46%) either because the difference between male and female were too small (even compared to that of *Dsx1*) or because their expression could not be correlated with the sex spectrum (Figure 3.5, also see Figure S1 for how binary and non-binary patterns were determined).

Unexpectedly, from the list of 731 sex-biased genes above, I could find only 8 genes showing significant difference between Line A male and Line B male (p-value < 0.05, absolute fold change ≥ 1.2, EDGE test) (Figure 3.6), which is a small number despite the distinct phenotypes of the two mutants.

3.3.4 Biological functions of the female- and male-biased genes

A simple hypergeometric test were carried out to determine which Gene Ontology (GO) terms were enriched in the obtained gene collection. My analysis showed that for the female-biased group, 109 GO biological process terms were over-presented while for the male-biased group this number was 176 (p-value < 0.05) (Table S2). Using the parent-child relationship of GO terms, all over-presented terms could be classified into 8 large categories: “embryonic development,” “reproduction,” “cell division,” “metabolism,” “transportation,” “signaling pathway,” “nucleic acid metabolism/modification,” and “other terms.” In each category, clear difference between female-biased and male-biased group coul be seen. The number of genes that were associated with “transportation” and “metabolism” in female-biased group were 113 (22.4%), much larger than that of the male-biased group which was 11 (4.9%). The opposite was found for “signaling pathway” and “embryonic development” categories (9 genes, 1.8% in female-biased against 33 genes, 14.6% in male-biased). I also noticed some common features between the two groups, for example chitin metabolism and several RNA-related gene expression regulation processes. However, the

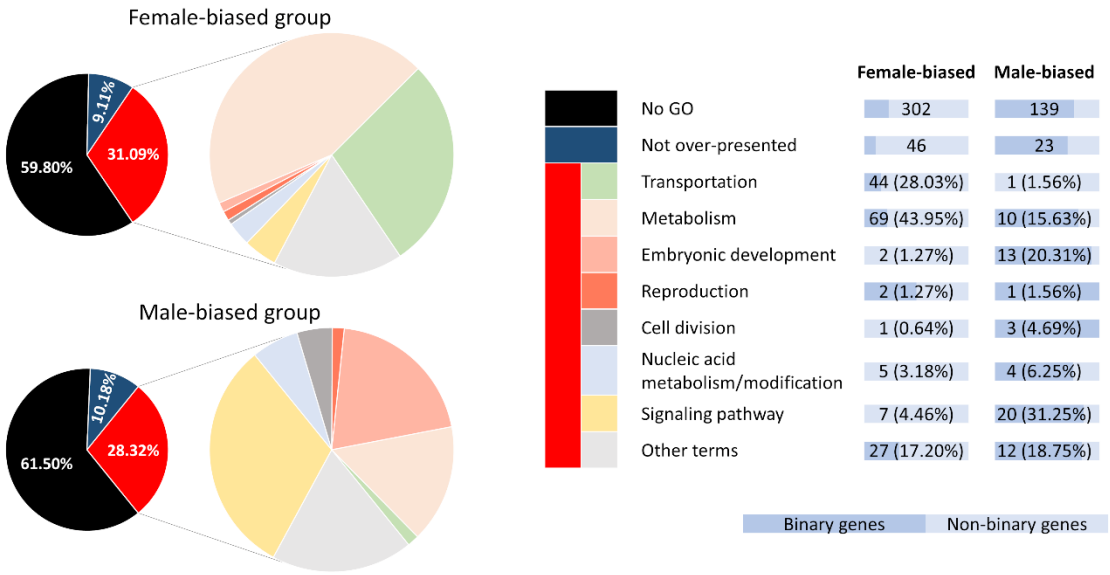

Figure 3.7: 731 sex-biased genes categorized into functional groups. Aside from genes found to be accounted for over-presence of certain GO terms (red group), the majority from this gene list are not associated with any GO terms (black group) while some other genes did not cause significant enrichment of the terms they are annotated with (dark blue group).

majority (around 60%) of the genes in the list could not be annotated with any GO term. Distribution of binary and non-binary genes among functional categories was rather even, resulting in dominance of non-binary genes in all female-biased categories and of binary genes in all male-biased categories (Figure 3.7).

3.3.5 Validation of RNA-seq gene expression with qPCR

To validate RNA-seq data, I picked several genes for qRT-PCR analysis (Figure 3.8). The same RNA samples that were prepared for RNA-seq were used in this experiment. Three genes from “male-biased, binary” set, 3 genes from “male-biased, non-binary” set, and 2 genes from “female-biased, non-binary” set were chosen. Among them are *Dsx1*, the mutated gene in this study, and *Dsx2*, another DM-domain gene of which male-biased expression has already been well described in D. magna [80]. Dapma7bEVm007306, an uncharacterized protein, was chosen because this gene is located at the same locus and downstream of

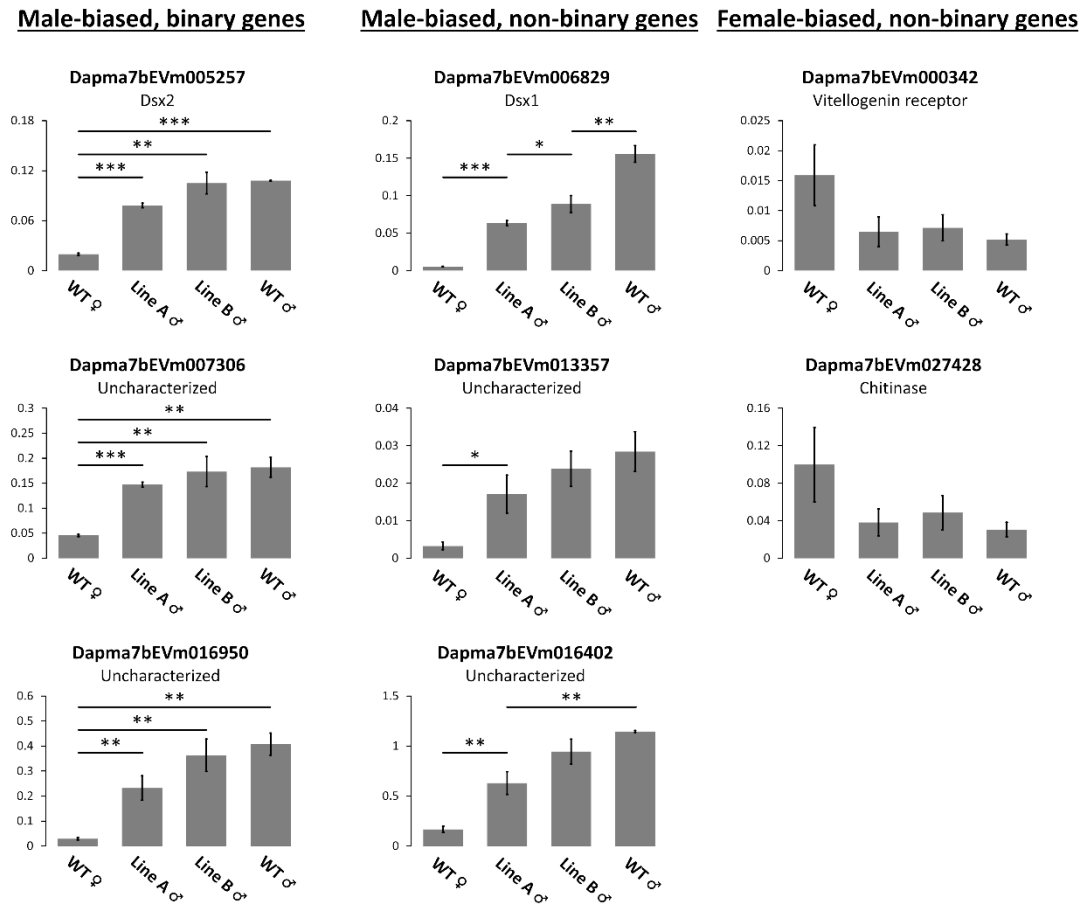

Figure 3.8: qRT-PCR of selected genes for validating RNA-seq expression. RNA samples of 40h embryos with triplicate for each group were used. All graphs show relative expression by normalization using the housekeeping ribosomal protein L32 gene. Error bars = SEM. * P < 0.05, ** P < 0.01, *** P < 0.001 (t-test).

Dsx1 and *Dsx2*. Three other genes, Dapma7bEVm013357, Dapma7bEVm016950 and Dapma7bEVm016402 (all are uncharacterized genes) are also found very close to each other in the same chromosome region (Figure 3.9). Dapma7bEVm000342 (a vitellogenin receptor) and Dapma7bEVm027428 (a chitinase) were chosen because they are potentially the downstream elements of *Dsx1* judging by their functions. Sex-bias could be confirmed in all cases while binary/non-binary pattern could be confirmed in 6/8 cases, indicating that my RNA-seq analysis is highly reliable.

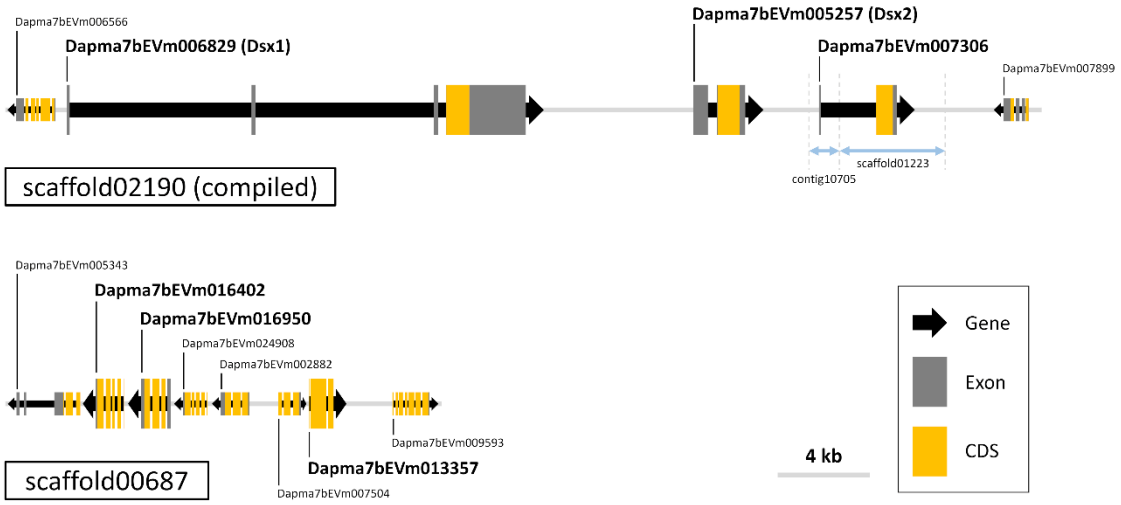

Figure 3.9: Two gene clusters showing sex-specific expression. Dapma7bEVm006829 (*Dsx1*) and Dapma7bEVm005257 (*Dsx2*) are two DM-domain genes whose male-biased expression has been well described previously. These two gene can be found next to each other on scaffold02190 of *D. magna* genome. According to my data, Dapma7bEVm007306, another gene located downstream of *Dsx2*, also showed male specific expression. A similar case was found on scaffold00687 where three neighboring genes, Dapma7bEVm016402, Dapma7bEVm016950 and Dapma7bEVm013357, also shared male-biased expression (see main text and Fig 3.8 for qPCR result). Be noted that Dapma7bEVm007396 is originally split-mapped on contig10705 and scaffold01223. However when comparing with *D. pulex* genome, I judged that these two fragments could be mapped to a long poly-n region between *Dsx2* and Dapma7bEVm007899, resulting in the compiled version of scaffold02190 as shown in this figure.

3.4 Discussion

Although sexual dimorphism can make male and female appear like two unrelated species, at genetic level, they differ only in genes on sex chromosome as in genetic sex determining species, or even in minuscule level if any as in environmental sex determining species. This similarity of genome between male and female may explain that sex change can happen naturally in several species [120,121]. These molecular and physiological evidence demonstrates that although sexual ambiguity is uncommon, it is a very natural manifestation of the genome and thus treating intersexes not as outliers but as an undeniable part of the population is very important. My data here has confirmed that in one more

species, *D. magna*, there are more to sex than just male and female and therefore the definition that sex is actually a spectrum can be applied to a much broader scale.

In contrast to extremely rare intersexuality in natural environment, I could develop a method to generate intersex phenotypes *D. magna* from the two modified genomes by simple chemical exposure. Previously, it was reported that intersex daphniids may appear under certain environmental setup such as high temperature [83]. However, non-genetic intersex-induction is inefficient and yields inconsistent result. My approach, on the other hand, focused on disrupting the key sex determining factor *Dsx1* of *D. magna* and therefore altered the entire sexual differentiation cascade downstream of *Dsx1*. Numerous studies have pointed out that DM-domain genes are involved in body wide somatic sexual development, from gonadal to non-gonadal and even neuronal tissues [26,104]. In *D. magna*, there are also evidence that *Dsx1* is required for the establishment of testis and many other male-specific structures [80], which is consistent with my observation in this chapter. Therefore, Line A and Line B represent intersex at whole body level and will serve as useful tools for the investigation into organogenesis of sexual traits as well as the creation of *D. magna* sex spectrum.

My RNA-seq data revealed a set of 449 genes correlated with *Dsx1* as their expression aligned to the sex spectrum given by the mutants, suggesting that these genes are downstream factors of *Dsx1*. Interestingly, the majority of these genes are negatively correlated (398 genes), which means they are directly or indirectly repressed by Dsx1, hence suggest an important role of Dsx1 as a transcriptional repressor in addition to a transcriptional activator. Another set of 282 genes exhibited sex-biased activity but their dimorphism was unaffected in the mutants. To explain, there are three possibilities. 1) These binary genes are less sensitive to *Dsx1* dosage than non-binary genes. 2) Genes annotated with categories related to transcription factor activity in the male-biased group function upstream of *Dsx1*. Epistatic relationship between *Dsx1* and these genes must be analyzed by their silencing, overexpression, and identification of Dsx1 binding sites. 3) These genes are under the control of another sex development pathway

independent of *Dsx1*, as in case of *Drosophila* the *fruitless* branch is recruited to establish sexual behavior in parallel with *doublesex* branch [122]. However, this is rather unlikely in *D. magna* because *Dsx1* RNAi induced complete feminization including production of offspring [80,123].

In the RNA-Seq analysis, female-biased group seemed to invest more to “transportation” and “metabolism” with the enrichment of many amino acid and carbohydrate biosynthetic processes. Male-biased group on the other hand showed the upregulation of a variety of “signaling pathways”. This result suggested that Dsx1 as a transcription factor had activated multiple signaling pathways to redirect organogenesis to male development, while at the same time as a repressor had slowed down metabolism. Because the majority (around 60%) of the genes in my list could not be annotated with any GO term (Figure 3.7), investigation into these unknown genes is necessary before any conclusion about *Dsx1* mode of action can be made.

Line A has a mutation of 6-bp deletion at start codon of *Dsx1* CDS and shows more severe feminization than Line B which harbors an intact *Dsx1* gene (Figure 2.5). Ribosomal scanning model suggests that deletion of the original start codon will force the translation to start from the second AUG, which may give rise to a mutated product in Line A. In this case, roughly 8% of amino acids will be truncated from N-terminus but the two conserved domains, DM-domain and oligomerization domain, will still remain intact. This may possibly alter the interaction of *Dsx1* to its binding target or to associated proteins, which reduces the performance of Dsx1 as a transcription factor. As many studies on *Drosophila* have pointed out, Dsx^F and Dsx^M may work in complexes such as dimers or heterodimers with other proteins to exert their sex- and tissue-specific functions [124–126]. As a complex, activity can be stabilized [127] and different complexes control different set of genes. Another possibility is that the truncation does not affect Dsx1 activity but translation from an alternative start site lacking simulating sequences has reduced the amount of translated protein. In mammalian, there is evidence that the *Dmrt1* gene is not dominant but dose sensitive [36] and therefore it can be expected that further reduction of Dsx1 amount would amplify

feminization effect. However, the situation can be much more complicated as translation initiated at suboptimal context is not only inefficient but may also lead to leaky scanning where other downstream AUGs will also be recognized at start sites [128]. This means in Line A, there is likely a mixture of active and inactive Dsx1 variants that compete with each other. To clarify the correct mechanism, direct qualification and quantification of Dsx1 protein with Western blot for example would be necessary.

It was intriguing to found that males of Line A developed ovotestes. Feminization of non-gonadal tissues such as first antennae, carapace curve and genital…, which are more or less quantitative traits, could be explained by the intermediate expression of the related sex differentiation genes due to weaken *Dsx1* activity. However, for gonads, the mechanism can be more complicated as this tissue features qualitative characteristics. It has been known that DM-domain genes are recruited in Sertoli cells which make up an important part of the somatic tissue in the testis and support differentiation of germ cells into sperms [102,105,106]. By observation of mCherry signal, I could confirm that *Dsx1* is also active in the gonads of Line A male and Line B male. However in Line A male, it is possible that while a duct system for transporting sperms was successfully established, oogenesis was not completely repressed, leading to generation of eggs without a gate for oviposition. Detailed histological characterization is needed to confirm this hypothesis.

Despite the evident difference in sexual phenotype between Line A and Line B (Figure 3.2), the number of gene differentially expressed between the two lines was very small (Figure 3.6). While these genes expressed at rather low level, there was one gene named Dapma7bEVm002034 (Endocuticle structural glycoprotein SgAbd-1) which seem to be more active than the others. Annotation of this gene suggesting its role in carapace formation, explaining why there was visible difference in rostrum and first antennae morphology between Line A and Line B males right at first swimming juvenile stage. Perhaps at the chosen stage, the *Dsx1*-related sex differentiation cascade is yet to be fully displayed. As a matter of fact, expression of *Dsx1* is temporally controlled and it is possible that

Dsx1 can target more genes in later stages as there is a surge in *Dsx1* activity during the transition from juvenile to adult (Section 2.3.6). In addition, to analyze more details of *Dsx1*-dependent transcriptional profile, enrichment of *Dsx1* positive tissues or cells would be needed.

Last but not least, the critical role of *Dsx1* as the central sex determining factor in *D. magna* is once again confirmed by this study. Consistent with previously published data in which embryonic knock-down of *Dsx1* by RNAi induced male to female reversal of gonadal and non-gonadal tissues [80], very similar effect could be found in the established mutants of this study. However, it is noteworthy that *Dsx2*, another DM-domain gene neighboring *Dsx1* that also has strong male-biased activity [80], was as well detected as a male-biased and binary gene in my analysis (Figure 3.8). Although the sex determining function of *Dsx2* was not proven by the similar RNAi experiment [80], a detailed expression analysis pointed out that *Dsx2* became more active toward the end of vitellogenesis cycle and during spermatogenesis, strongly suggest a distinctive role of *Dsx2* in the sexual development of *D. magna* [129]. Here, I do not eliminate the possibility that *Dsx1* activity was actually extinguished in Line A and it was other factors such as *Dsx2* that built up male-like features in Line A male.

3.5 Data availability

The RNA-seq data generated in this chapter were deposited in NCBI's Gene Expression Omnibus (GEO) and can be accessed through the accession number of GSE150820.

CHAPTER 4: CHARACTERIZATION OF ISOLATED DSX1-ACTIVE CELLS

4.1 Introduction

To execute the sex- and tissue-specific function, DM-domain genes are known to cooperate with a variety of cofactors. For example in *Drosophila*, Intersex (Ix) and Hermaphrodite (Her) are two well-known sex-nonspecific proteins that cooperate with Dsx^F in shaping the female body. Dsx^F and Dsx^M also work in combination with bZIP to promote and repress transcription of the fat body, respectively [124]. Likewise, Dsx^F is recruited by the Hox transcription factor Abdominal-A (Abd-B) to induce apoptosis of neuroblasts required for male mating behavior [126]. On top of that, judging from their localized expression, the DM-domain genes themselves is supposed to be under the control of non-dimorphic spatiotemporal patterners as well. In *Drosophila*, there is evidence that *Dsx* is not only a cofactor but also one of the targets of the Hox gene *Abd-B* [130]. In *Daphnia magna*, *Dsx1* is activated time-specifically by *Vrille* only during early embryogenesis [81]. Therefore, it can be seen that both sex determination and sex differentiation do not principally depend on dimorphic switches alone, but are also controlled by non-dimorphic factors.

Because of that, with whole body characterization of sex-biased genes only, a crucial part of *Dsx1* interactome would be overlooked. It is necessary to analyze the transcriptome of isolated tissues and cells also in order to decode the *Dsx1* pathway of *D. magna*. In this chapter, I propose a protocol for isolation *Dsx1*-active cells from 40 h embryos by making use of the *mCherry* reporter in Line B. Single cells were derived from 40 h Line B male embryos and those with strong red fluorescence were isolated using Fluorescence Activated Cell Sorting (FACS). Transcriptome of each cell was sequenced separately using the C1 CAGE (Cap Analysis Gene Expression (CAGE) of single cells captured by C1 Fluidigm system) protocol to explore the cell types present in the isolated *Dsx1*-active cell

population. This experiment was still at a preliminary stage and optimization of the methods is required. However I expect that when successful, obtained data will be of great use for the discovery of *Dsx1* mechanism.

4.2 Materials and Methods

4.2.1 *Daphnia* culturing and male production

Only Line B was used in this chapter. Culturing conditions and male production by Fenoxycarb was the same as described in Chapter 3 (Section 3.2.1).

4.2.2 Derivation of single cells from *Daphnia* embryos

First, embryos were synchronized by halting development of earlier ovulated eggs at 4 °C (see Section 3.2.3). After synced, mothers with embryos were culture normally until the age of interest.

For embryonic cell derivation, embryos from 5–10 mothers were pooled as one sample (too many embryos may lead to overload and reduce efficiency). After removed from mothers and transferred to 1.5 mL tube, embryos were washed two times with 200 µL MGM450 (Modified Grace's Medium, an insect cell culture medium) supplemented with 1% BSA (Bovine Serum Albumin). Then, the medium was replaced by 200 µL 0.25% Trypsin in PBS (Phosphate-buffered Saline) and embryos were gently homogenized using an automated micropestle until no large tissue clump remained. Homogenate was left at room temperature for 10 min to allow trypsinization to happen before 600 µL of MGM450 supplemented with 10% FBS (Fetal Bovine Serum) was added to inactive the enzyme. The mixture was pipetted gently to disintegrate sticky cell clumps and filtered through a 40 µm cell strainer. Additional 400 µL of MGM450 + 1% BSA was used to wash cells that still stuck on strainer mesh, resulted in approximately 1.2 mL of cell filtrate. Cells were pelleted at 700 *g*, 4 °C for 1 min, then resuspended in 200–1000 µL of MGM450 + 1% BSA (depends on the input amount of embryos). This clean cell suspension was kept on ice before proceeding to downstream experiments.

4.2.3 Flow cytometry analysis and fluorescence activated cell sorting

Cells suspension obtained from Section 4.2.2 was directly used as inject for flow cytometry analysis and cell sorting. Flow cytometry was performed using a CytoFLEX S system (Beckman Coulter) for preliminary evaluation of cell sample. Sorting of cells was performed at Osaka University Immunology Frontier Research Center (IFReC, Osaka, Japan) with the help of specialists. See Results section for details of gating.

4.2.4 Total RNA extraction and qRT-PCR

After sorting, cells were pelleted at 700 *g*, 4 °C for 5 min. Medium was pipetted out until a small amount of liquid remained to avoid loss of cells. Cell samples were then transferred to liquid nitrogen for flash-freezing. RNA extraction was performed by using Sepasol-RNA I solution (Nacalai Tesque, Kyoto, Japan), followed by phenol-chloroform purification and DNase treatment. Because of the small amount of sample, 10 µg of yeast tRNA was added to each sample together with Sepasol-RNA I to assist the extraction process. qRT-PCR was done as described in previous chapters (Section 3.2.4).

4.2.5 C1 CAGE

Capturing of single cells using C1 Fluidigm and CAGE library generation was done by collaborators.

4.2.6 CAGE data analysis

Mapping of sequenced libraries was done using CLC Genomics Workbench software (Qiagen) as described in Chapter 3 (Section 3.2.6).

4.3 Results

4.3.1 Establishment of a method for deriving cells from embryos

Until now, except for some few attempts, there is almost no decent work on *Daphnia* cell culture [131]. Due to the lack of a platform for derivation and in vitro culturing of cells for this species, I adapted the commonly used protocol that

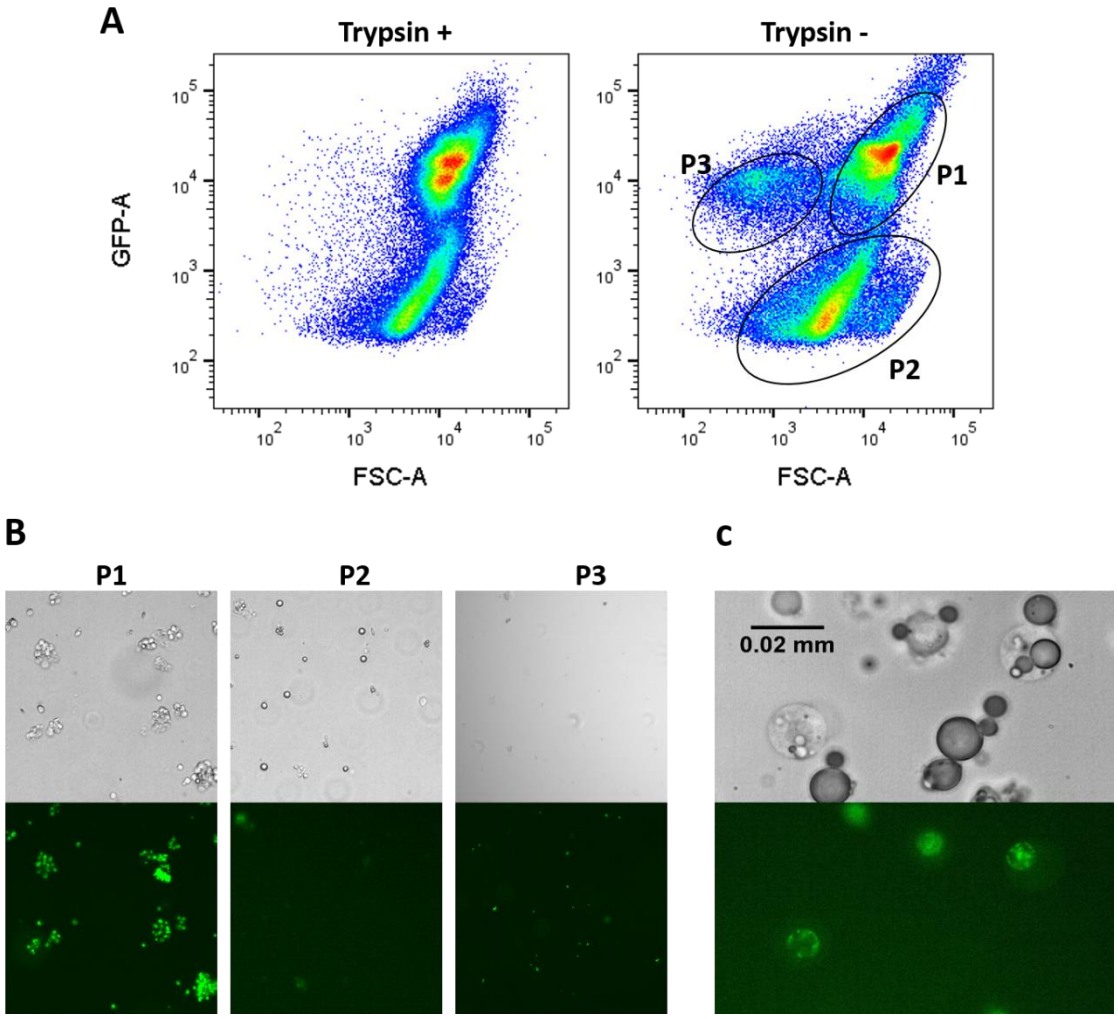

Figure 4.1: Flow cytometry analysis of derived embryonic cell sample. (A) Using the cell derivation protocol established in this study, typically three populations will present in the final suspension: P1 – intact cell, P2 – lipid drops and P3 – small debris from burst cells or yolk protein. Implement of trysinization improved number of cells in P1 and eliminate P3. **(B)** Each population from panel A observed under microscope. EGFP signal (from HG2E background genotype) can be used to easily distinguish the three populations. Intact cells are round in shape and show strong green fluorescence. Lipid drops are also round but glossier and do not have fluorescence. Debris appear as tiny bits and some have fluorescence. **(C)** A close-in of some cells. Localization of EGFP signal in nuclei can be seen.

involves manual homogenization and trypsinization of whole embryo (see Section 4.2.2 for detailed protocol). As the cells will be used for sorting and transcriptome analysis soon after derivation, I only focused on cell integrity and do not experimented on culturing conditions. That is why some steps are omitted from

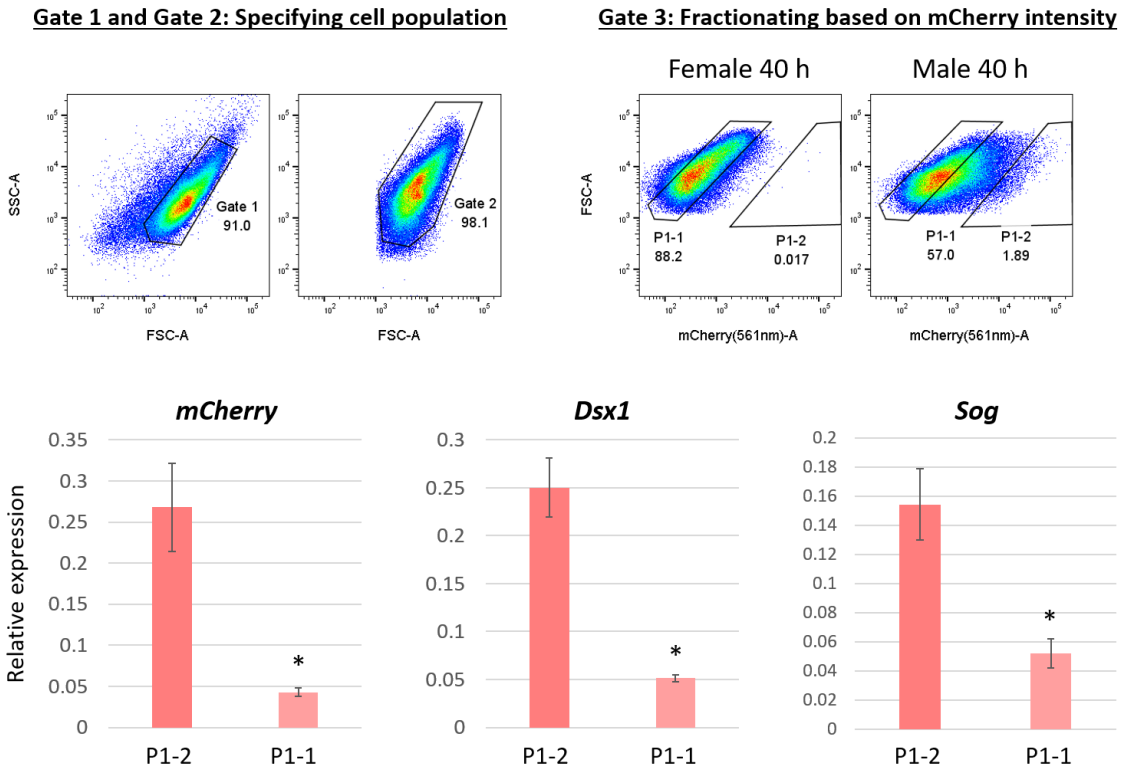

Figure 4.2: Enrichment of Dsx1-active cells from Line B male embryos by FACS. 40 hpo male embryos of Line B were used for cell derivation and proceeded to FACS. Cells expressing strong mCherry signal were sorted by a combination of three gates (description in main text). Graphs on bottom rows show expression level normalized with L32. *p < 0.01 (t-test).

the protocol such as sterilization or the use of antibiotics. By observation of cells under microscope, I confirmed that in the final cell sample, a fair amount of single cells could be obtained. In the samples, impurities such as lipid drops and small debris, probably from burst cells and yolk protein also presented. However they can be distinguished easily by flow cytometry due to very different light scattering and fluorescence properties from intact cells. Especially, the use of trypsin could improve collected cell amount by at least 3 times and help remove small debris (Figure 4.1).

4.3.2 Establishment of a FACS method for enriching *Dsx1*-active cells

In this chapter, I used 40 hpo Line B male embryos with the same reason explained in Chapter 3 (Section 3.3.3). To isolate cells that strongly express *Dsx1*

from male embryos of Line B by FACS, I used a combination of three gates. The first gate specifies the major population with homogeneous FSC to SSC properties. Second gate specifies the population with higher FSC and higher EGFP signal. These two gates help define the true cell population and eliminate unwanted particles such as lipid drops or cell clumps. In the third gate, I specified a 2% cell fraction that showed highest mCherry signal (mCherry-positive cell fraction) as the target for further analysis (Figure 4.2A, P1-2).

First, to confirm whether Dsx1-active cells were actually enriched after FACS, another cell fraction that was similar with female cells (Figure 4.2A, P1-1) was also collected from the same sample and used as negative control to compare with mCherry-positive fraction by qPCR. As this control fraction takes up roughly 60% of the total cell population, it is reasonable to assume that it can also represent the full population. Indeed, by referring to qPCR data from previous chapters where *mCherry* and *Dsx1* relative expression was at around 0.06–0.08 in 40 h male embryos (Figure 3.3A and Figure 3.8), such values obtained for fraction P1-1 was comparable which was 0.043 ± 0.005 for *mCherry* and 0.051 ± 0.004 for *Dsx1*. As a result, I found that mRNA level of *mCherry* and *Dsx1* in mCherry-positive cell fraction was higher than control fraction by 6.3 fold and 4.9 fold respectively, indicating that the use of FACS with the chosen gating setup could successfully isolate Dsx1-active cells. As *Dsx1* is mostly localized to tissues of ventral field, I also checked the expression level of a ventral specification gene *Sog* (short gastrulation) and found that mRNA level of this gene was also 2.97 fold higher in the mCherry-positive cell fraction (Figure 4.2 B). These data suggested that, samples collected by the established protocol could be used to characterize the asymmetric interaction of *Dsx1* with sex-nonspecific factors.

4.3.3 Single cell transcriptome analysis of Dsx1-active cells

This experiment was done in collaboration under the “先進ゲノム支援” project. Right after sorting for Dsx1-active cells, sample were transported on ice and subjected to single cell capturing and library generation as soon as possible. CAGE sequencing was performed in two runs, 96 samples (including two bulks)

for 1st run and 49 samples (including one bulk) for 2nd run. Average 3 million paired reads were generated for each sample and some samples had up to 8 million reads. As a result of mapping, for 1st run roughly 11% of reads were mapped to spike-ins and for 2nd run the ratio was 40%. 58% and 42% of reads could be mapped to *D. magna* genome for 1st run and 2nd run, respectively, resulted in only 1–2 million reads were relevant for each sample of both runs. Furthermore, 45% (1st run) and 67% (2nd run) of these relevant reads originated from rRNA, indicating that sequencing depth might be too low to correctly quantify weak-expressing genes. In fact, *Dsx1* was almost undetectable in all samples. Thus, I did not proceed as further analysis would lead to unreliable results.

4.4 Discussion

In this chapter, I introduced a protocol for isolation of *D. magna* embryonic cells showing strong Dsx1 activity, or in other words the subset of cells that are masculinized, which was made possible thank to the *mCherry* reporter of Line B. Targeted characterization of sex-specific tissues is important to unfold the mechanisms of sex-determining switch like *Dsx1*, for example how *Dsx1* is recruited to a tissue and how this gene specifically control the sex differentiation of that tissue differently than it would elsewhere. Crosstalk of *Dsx1* with non-dimorphic cascade such as body planning and organogenesis also may become clear using this approach. Although very small, isolation of tissues in adult *D. magna* is not impossible. For example, transcriptomes of ovaries in JH sensitive period has been characterized before [132]. However, in early embryos where patterning of rudiment body parts are the strongest, isolation of embryonic tissues would be very tedious without a good marker. In Line B, because Dsx1-active cells is labelled with mCherry fluorescence, it is possible to use this mutant to obtained masculinized cells at any stage of development with the help of FACS.

The ultimate goal of this chapter was to annotate the cell types present in isolated Dsx1-active cell population through single cell transcriptomic analysis. However, due to lack of experience in handling *D. magna* cells, fruitful results were not acquired for the moment. The C1 CAGE protocol that we applied was

optimized for cultured mammalian cells [133], whose properties must be very different from *D. magna* embryonic cells. In fact, it seemed that our *D. magna* cells were significantly smaller than common mammalian cell lines, resulted in uncertainty during single cell capturing. Other factors that need to be optimized for C1 CAGE protocol includes adjustment of spike-ins and sequencing depth to solve the problem of over-presented rRNA reads. Nevertheless, data obtained in this chapter will be useful as reference for future designs of experiments.

CHAPTER 5: DISCUSSION

The importance of unfolding molecular mechanism of sexual development

Sex and sexual reproduction is a fascinating phenomenon of the living world. As the standard barrier between species is reproduction, it is not overstating when we say that there a specific sexual development system for every species. Intriguingly, it seems that however divergence sexual development might have become, segregation of sex into male and female is an unchanged principle. This indicates that there exists a core of sexual molecular network that is essentially conserved through the long history of evolution. Elucidating this molecular core is important as it might hold the key to answer many pending questions: 1) How has sex evolved? Were there male and female from the beginning? Or was sex arise from an ability to transform the body to adapt to the environment, later chosen as a reproductive strategy? 2) If male and female are the ultimate choice of evolution, why do intersex individuals keep appearing? Is intersexuality normal, like a common mole on our skin that makes everyone more charming, or is it like a tumor that is harmful to the population and need to be repaired? As different answers will lead to different scientific and social conceptualizations, a correct one is of most necessity.

Why *Daphnia* is an influential model for the study of sex

The cycloparthenogenetic reproduction of *Daphnia* is unique in that sexual reproduction is completely ecoresponsive. In this clade of animal, sex is less a mean of creating next generation but more an adaptive strategy for survival. Generally, *Daphnia* is accepted as an ancient species that is closely related to common crustacean ancestor, closer than the insect model *Drosophila*. This can be explained by the ability of *Daphnia* to create resting eggs that can undergo dormancy for decades or even longer, thus serve as an old genotype storage that can contribute back to newer genomes [65]. Despite the antiquity, it is still under debate whether the environmental sex determination and parthenogenesis of

Daphnia are modern or ancient traits. By looking into genomic regions responsible for male production, a study has pointed out that within the *Daphnia* clade, transition from ESD to partial GSD occurred in the past [134], implying that ESD was the older form of sex. Although more work still need to be done, clarifying the position of *Daphnia* sex in evolution would provide valuable data for understanding the nature and logic of sexual development.

Why focus on the DM-domain gene family

As mentioned in Introduction, DM-domain genes are conserved not only in sequence but also in their function during sexual development. However, the position of this gene in the sex cascade varies greatly among species [135]. In some, DM-domain gene acts as a sex determinant, while in others, it belongs to sex differentiation process. In some cases, even between two closely related species, DM-domain gene is found in sex cascade of one but not the other. Therefore, it is difficult to conclude whether this gene family is the beginning of sex or on the contrary subsequently recruited after the sex cascade had already formed.

Aside from their role in sexual development, another common feature of this gene family can be found in the embryonic expression. In arthropods, DM-genes can be group into two sets, the sex determining Dsx-like set whose embryonic expression seems to be derivative, and the remaining Dmrt-set whose embryonic expression was found to be highly conserved [136]. Similarly in vertebrates, among many Dmrt subfamilies, sex-related functions is confirmed for Dmrt1 only, while others are important in somitogenesis and neurodevelopment [137]. Therefore, it has been suggested that the sexual role of some DM-domain genes was later acquired after duplication from a predecessor that originally belonged to embryonic developmental pathway. Exploring other non-sexual functions of this gene family would shed light on how they have become involved in sexual development and provide insights into the origin of sex.

How this study helped expand understandings about *D. magna* sexual development

Previously, the role of *Dsx1* as a masculinizing factor was discovered by knock-down and overexpression data [80]. In this study, by generating two different mutants, Line B in which *Dsx1* was hemizygously knock-out, and Line A in which on top of hemizygous knock-out, the coding sequence on remaining allele was mutated, this role of *Dsx1* was once again confirmed. Due to the presence of *Dsx1* in probably all male-specific structures around the body (Chapter 2) and simultaneous feminization of those structures when this gene was mutated (Chapter 3), it can be inferred that *Dsx1* dictates sex differentiation by directly affecting multiple downstream target, meaning that in *D. magna Dsx1* stays at the bottom of sex determination cascade similar to *Drosophila*. Interestingly, my observation of *Dsx1* in embryogenesis revealed that its expression resemble that of the Dmrt11E group (not the Dsx-like group) of arthropods and Dmrt2 group of vertebrates (Chapter 2), suggesting the involvement of this gene in embryonic body planning and thus further emphasize the intriguing position of *D. magna* sex in evolution.

The discovery of non-binary nature of a large proportion of *Dsx1* downstream genes (Chapter 3) implies that many *D. magna* sexual traits are built from bipolar stabilization of a morphologically plastic features. This means *D. magna* sexual development cascade support the sex spectrum hypothesis. However, as I had hoped to find more binary genes that completely switch states in mutants, I was not able to. Through observation in Line A male, some dimorphic traits seemed to get feminized more severely than the others. For example accumulation of yolk protein into gonads is rather biased compared to the moderately shortened first antennae. Therefore some genes must have been completely bended from male to female position in the male mutants. If such genes is found, we may be able to say that while the sex spectrum idea is justifiable, it may not be applied to one hundred percent of sexual features.

To sum up, data from this study highlighted that the binary activity of *Dsx1* is a crucial but not absolute factor for establishing and maintaining sexual identity of daphniid, meaning that sex differentiation genes downstream genes of Dsx1

may break free from the binary control under certain conditions to give rise to intersexuality.

How this study will contribute to future research

Two maintainable mutants created in this study, Line B as a reporter for *Dsx1* activity and Line A as source for stable production of intersex daphniids, will surely serve as powerful tool to facilitate further research into *Daphnia* sexual development. For instance, Line B can be used for quick screening of *Dsx1* regulators. Usually, quantifying *Dsx1* using the tedious qRT-PCR protocol is required to evaluate post-manipulation of selected gene (knock-out, knock-down, etc.). Using Line B, the red fluorescence is a convenient indicator that can replace qPCR and speedup the process. In fact, Line B has been used this way in some published works [81,123]. Likewise, by using mCherry for tracking Dsx1 dynamic progress in Line A and Line B, cellular mechanism of sexual organogenesis can be unfold. It is still unclear in *D. magna* that male structures are completely consisted of Dsx1-active cells or some sexually neutral cells also coexist. Also, whether Dsx1-active cells can induce sexual differentiation of nearby cells (through signal molecules for example) is needed to be investigated.

The RNA-seq data obtained in this study is also a useful resource for selecting upstream and downstream candidates for *Dsx1* cascade. In term of engineering, *D. magna Dsx1* cascade is interesting in many aspects. First, it is a molecular circuitry for converting environmental cues to physiological response. This means, a combination of molecular sensors for abiotic and biotic factors can be identified. Second, varying input signals can be stabilize into binary output. For example, when exposed to JH analogs at sub-optimal concentration, a mixture of male and female but not intersex will be produced from the brood. This indicates that in the signal relaying process, there are elements that act as amplifiers and thresholders to regulate the intensity of relayed signal. And third, although the sensitive window for JH is very narrow (a 6-hour duration during oogenesis), output signal (*Dsx1* expression) is permanent. This means there must be a signal looping recruited to maintain the message when the input signal is gone. In most

inducible transgene expression systems, activity of target gene relies on the presence of inducer in dose-dependent manner. In contrast, the *Dsx1* circuitry offer a novel concept in which varying and transient inducer can trigger permanent and stable response of target gene which can be useful for application. For instance, in our lab, *Daphnia* is being engineered as sensor models for water quality assessment. However, in the most common approach where coupling of a sensor and its direct target modified to become the reporter, weak or unstable in reporting ability is usually observed. With the knowledge of *D. magna* innate sensors as well as amplifiers, thresholders and maintenance loop, it can be foreseen that we can engineer this animal in a more robust way to develop stronger and versatile reporter strains.

Last but not least, as the idea of sex spectrum is becoming more and more accepted, there comes along a need to search for a method to quantify the sexual status of each individual. Since morphology, karyotype or hormonal level… are now considered to be not 100% reliable anymore and may lead to false assumption of one's sex, it is necessary to establish a comprehensive set of molecular markers that can help interpret sexuality precisely. One of the idea is to use the whole transcriptome as the marker from which equilibrium state of sexual development genes will serve as a measurable parameter. To achieve this goal, more exhaustive characterization of intersexes like what have been done in this study is still required.

Concluding remarks

By creation and characterization of two modified genotype related to *Dsx1*, a *Dsx1*-reporter and an intersex, this study on one hand provide new insights into the cellular and molecular basis of *Daphnia magna* sex spectrum, on the other hand establish powerful tools that facilitate further investigation into the mysterious environmental sex determination of this species.

References

1. Barton NH. Why sex and recombination? Cold Spring Harb Symp Quant Biol. 2009;74: 187–195. doi:10.1101/sqb.2009.74.030

2. Bengtsson BO. Lost Sex. Schön I, Martens K, Dijk P, editors. Lost Sex. Dordrecht: Springer Netherlands; 2009. doi:10.1007/978-90-481-2770-2

3. Williams TM, Carroll SB. Genetic and molecular insights into the development and evolution of sexual dimorphism. Nat Rev Genet. 2009;10: 797–804. doi:10.1038/nrg2687

4. Ford AT. Intersexuality in Crustacea: An environmental issue? Aquat Toxicol. 2012;108: 125–129. doi:10.1016/j.aquatox.2011.08.016

5. Pereira R, Narita S, Kageyama D, Kjellberg F. Gynandromorphs and intersexes: potential to understand the mechanism of sex determination in arthropods. Terr Arthropod Rev. 2010;3: 63–96. doi:10.1163/187498310X496190

6. Lambeth LS, Smith CA. Disorders of sexual development in poultry. Sex Dev. 2012;6: 96–103. doi:10.1159/000334059

7. Bahamonde PA, Munkittrick KR, Martyniuk CJ. Intersex in teleost fish: Are we distinguishing endocrine disruption from natural phenomena? Gen Comp Endocrinol. 2013;192: 25–35. doi:10.1016/j.ygcen.2013.04.005

8. Villagómez DAF, Parma P, Radi O, Di Meo G, Pinton A, Iannuzzi L, et al. Classical and molecular cytogenetics of disorders of sex development in domestic animals. Cytogenet Genome Res. 2009;126: 110–131. doi:10.1159/000245911

9. Hull CL, Fausto-Sterling A. How sexually dimorphic are we? Review and synthesis. Am J Hum Biol. 2003;15: 112–116. doi:10.1002/ajhb.10122

10. Harper C. Intersex. Berg; 2007. doi:10.4324/9781003103554

11. Hyde JS, Bigler RS, Joel D, Tate CC, van Anders SM. The future of sex

and gender in psychology: Five challenges to the gender binary. Am Psychol. 2019;74: 171–193. doi:10.1037/amp0000307

12. Hodgkin J. Primary sex determination in the nematode C. elegans. Development. 1987;101: 5–16.

13. Baker BS, Ridge KA. Sex and the single cell. I. On the action of major loci affecting sex determination in Drosophila melanogaster. Genetics. 1980;94: 383–423.

14. Ainsworth C. Sex redefined. Nature. 2015;518: 288–291. doi:10.1038/518288a

15. Lillie FR. Sex-determination and sex-differentiation in mammals. Proc Natl Acad Sci. 1917;3: 464–470. doi:10.1073/pnas.3.7.464

16. Bachtrog D, Mank JE, Peichel CL, Kirkpatrick M, Otto SP, Ashman T-L, et al. Sex determination: Why so many ways of doing it? PLoS Biol. 2014;12: e1001899. doi:10.1371/journal.pbio.1001899

17. Berec L, Schembri PJ, Boukal DS. Sex determination in Bonellia viridis (Echiura: Bonelliidae): Population dynamics and evolution. Oikos. 2005;108: 473–484. doi:10.1111/j.0030-1299.2005.13350.x

18. Casas L, Saborido-Rey F, Ryu T, Michell C, Ravasi T, Irigoien X. Sex change in clownfish: Molecular insights from transcriptome analysis. Sci Rep. 2016;6: 35461. doi:10.1038/srep35461

19. Bear A, Monteiro A. Both cell-autonomous mechanisms and hormones contribute to sexual development in vertebrates and insects. BioEssays. 2013;35: 725–732. doi:10.1002/bies.201300009

20. Bergerard J. Environmental and physiological control of sex determination and differentiation. Annu Rev Entomol. 1972;17: 57–74. doi:10.1146/annurev.en.17.010172.000421

21. Werren JH, Baldo L, Clark ME. Wolbachia: master manipulators of

invertebrate biology. Nat Rev Microbiol. 2008;6: 741–751. doi:10.1038/nrmicro1969

22. Baroiller JF, D’Cotta H, Saillant E. Environmental effects on fish sex determination and differentiation. Sex Dev. 2009;3: 118–135. doi:10.1159/000223077

23. Shen Z-G, Wang H-P. Environmental sex determination and sex differentiation in teleosts - How sex is established. Sex Control in Aquaculture. Chichester, UK: John Wiley & Sons, Ltd; 2018. pp. 85–115. doi:10.1002/9781119127291.ch4

24. Rich AL, Phipps LM, Tiwari S, Rudraraju H, Dokpesi PO. The increasing prevalence in intersex variation from toxicological dysregulation in fetal reproductive tissue differentiation and development by endocrine-disrupting chemicals. Environ Health Insights. 2016;10: EHI.S39825. doi:10.4137/EHI.S39825

25. Eagly AH, Wood W. The nature–nurture debates. Perspect Psychol Sci. 2013;8: 340–357. doi:10.1177/1745691613484767

26. Kopp A. Dmrt genes in the development and evolution of sexual dimorphism. Trends Genet. 2012;28: 175–184. doi:10.1016/j.tig.2012.02.002

27. Verhulst EC, van de Zande L. Double nexus--Doublesex is the connecting element in sex determination. Brief Funct Genomics. 2015;14: 396–406. doi:10.1093/bfgp/elv005

28. Hildreth PE. Doublesex, recessive gene that transforms both males and females of Drosophila into intersexes. Genetics. 1965;51: 659–78.

29. Shen MM, Hodgkin J. mab-3, a gene required for sex-specific yolk protein expression and a male-specific lineage in C. elegans. Cell. 1988;54: 1019–1031. doi:10.1016/0092-8674(88)90117-1

30. Prakash A, Monteiro A. Molecular mechanisms of secondary sexual trait

development in insects. Curr Opin Insect Sci. 2016;17: 40–48. doi:10.1016/j.cois.2016.06.003

31. Yi W, Ross JM, Zarkower D. mab-3 is a direct tra-1 target gene regulating diverse aspects of C. elegans male sexual development and behavior. Development. 2000;127: 4469–4480.

32. Ferguson-Smith M. The evolution of sex chromosomes and sex determination in vertebrates and the key role of DMRT1. Sex Dev. 2007;1: 2–11. doi:10.1159/000096234

33. Ge C, Ye J, Zhang H, Zhang Y, Sun W, Sang Y, et al. Dmrt1 induces the male pathway in a turtle species with temperature-dependent sex determination. Development. 2017;144: 2222–2233. doi:10.1242/dev.152033

34. Blackless M, Charuvastra A, Derryck A, Fausto-Sterling A, Lauzanne K, Lee E. How sexually dimorphic are we? Review and synthesis. Am J Hum Biol. 2000;12: 151–166. doi:10.1002/(sici)1520-6300(200003/04)12:2<151::aid-ajhb1>3.0.co;2-f

35. Baker BS, Hoff G, Kaufman TC, Wolfner MF, Hazelrigg T. The doublesex locus of Drosophila melanogaster and its flanking regions: A cytogenetic analysis. Genetics. 1991;127: 125–138.

36. Krentz AD, Murphy MW, Kim S, Cook MS, Capel B, Zhu R, et al. The DM domain protein DMRT1 is a dose-sensitive regulator of fetal germ cell proliferation and pluripotency. Proc Natl Acad Sci. 2009;106: 22323–22328. doi:10.1073/pnas.0905431106

37. Capel B. Vertebrate sex determination: evolutionary plasticity of a fundamental switch. Nat Rev Genet. 2017;18: 675–689. doi:10.1038/nrg.2017.60

38. Fryer G. Functional morphology and the adaptive radiation of the Daphniidae (Branchiopoda: Anomopoda). Philos Trans R Soc London Ser

B Biol Sci. 1991;331: 1–99. doi:10.1098/rstb.1991.0001

39. Martin JW, Davis GE. An updated classification of the recent Crustacea. Natural History Museum of Los Angeles County Los Angeles; 2001.

40. Glenner H, Thomsen PF, Hebsgaard MB, Sørensen MV, Willerslev E. The origin of insects. Science (80-). 2006;314: 1883–1884. doi:10.1126/science.1129844

41. Schwentner M, Combosch DJ, Pakes Nelson J, Giribet G. A phylogenomic solution to the origin of insects by resolving crustacean-hexapod relationships. Curr Biol. 2017;27: 1818-1824.e5. doi:10.1016/j.cub.2017.05.040

42. Miner BE, De Meester L, Pfrender ME, Lampert W, Hairston NG. Linking genes to communities and ecosystems: Daphnia as an ecogenomic model. Proc R Soc B Biol Sci. 2012;279: 1873–1882. doi:10.1098/rspb.2011.2404

43. Qi W, Nong G, Preston JF, Ben-Ami F, Ebert D. Comparative metagenomics of Daphnia symbionts. BMC Genomics. 2009;10: 172. doi:10.1186/1471-2164-10-172

44. Grossart H-P, Dziallas C, Leunert F, Tang KW. Bacteria dispersal by hitchhiking on zooplankton. Proc Natl Acad Sci. 2010;107: 11959–11964. doi:10.1073/pnas.1000668107

45. Freese HM, Schink B. Composition and stability of the microbial community inside the digestive tract of the aquatic crustacean Daphnia magna. Microb Ecol. 2011;62: 882. doi:10.1007/s00248-011-9886-8

46. Eckert EM, Pernthaler J. Bacterial epibionts of Daphnia: a potential route for the transfer of dissolved organic carbon in freshwater food webs. ISME J. 2014;8: 1808–1819. doi:10.1038/ismej.2014.39

47. Peerakietkhajorn S, Kato Y, Kasalický V, Matsuura T, Watanabe H. Betaproteobacteria L imnohabitans strains increase fecundity in the

crustacean D aphnia magna: symbiotic relationship between major bacterioplankton and zooplankton in freshwater ecosystem. Environ Microbiol. 2016;18: 2366–2374. doi:10.1111/1462-2920.12919

48. Laforsch C. Extreme helmet formation in Daphnia cucullata induced by small-scale turbulence. J Plankton Res. 2004;26: 81–87. doi:10.1093/plankt/fbg114

49. Weiss LC, Albada B, Becker SM, Meckelmann SW, Klein J, Meyer M, et al. Identification of Chaoborus kairomone chemicals that induce defences in Daphnia. Nat Chem Biol. 2018;14: 1133–1139. doi:10.1038/s41589-018-0164-7

50. Pijanowska J. Cyclomorphosis in Daphnia: an adaptation to avoid invertebrate predation. Hydrobiologia. 1990;198: 41–50. doi:10.1007/BF00048621

51. Tollrian R. Chaoborus crystallinus predation on Daphnia pulex: can induced morphological changes balance effects of body size on vulnerability? Oecologia. 1995;101: 151–155. doi:10.1007/BF00317278

52. Weber RE, Vinogradov SN. Nonvertebrate hemoglobins: Functions and molecular adaptations. Physiol Rev. 2001;81: 569–628. doi:10.1152/physrev.2001.81.2.569

53. Kimura S, Tokishita S, Ohta T, Kobayashi M, Yamagata H. Heterogeneity and differential expression under hypoxia of two-domain hemoglobin chains in the water flea, Daphnia magna. J Biol Chem. 1999;274: 10649–10653. doi:10.1074/jbc.274.15.10649

54. Martins J, Oliva Teles L, Vasconcelos V. Assays with Daphnia magna and Danio rerio as alert systems in aquatic toxicology. Environ Int. 2007;33: 414–425. doi:10.1016/j.envint.2006.12.006

55. OECD. Test No. 202: Daphnia sp. Acute Immobilisation Test. OECD; 2004. doi:10.1787/9789264069947-en

56. OECD. Test No. 211: Daphnia magna Reproduction Test. OECD; 2012. doi:10.1787/9789264185203-en

57. Hebert PDN. The population biology of Daphnia (Crustacea, Daphnidae). Biol Rev. 1978;53: 387–426. doi:10.1111/j.1469-185X.1978.tb00860.x

58. Zaffagnini F. Reproduction in Daphnia. Mem Ist Ital Idrobiol. 1987;45: 245–284.

59. LeBlanc GA, Medlock EK. Males on demand: the environmental-neuro-endocrine control of male sex determination in daphnids. FEBS J. 2015;282: 4080–4093. doi:10.1111/febs.13393

60. Camp AA, Haeba MH, LeBlanc GA. Complementary roles of photoperiod and temperature in environmental sex determination in Daphnia spp. J Exp Biol. 2019;222: jeb195289. doi:10.1242/jeb.195289

61. Kleiven OT, Larsson P, Hobæk A, Hobaek A. Sexual reproduction in Daphnia magna requires three stimuli. Oikos. 1992;65: 197. doi:10.2307/3545010

62. Mellors WK. Selective predation of ephippal Daphnia and the resistance of ephippal eggs to digestion. Ecology. 1975;56: 974–980. doi:10.2307/1936308

63. Möst M, Chiaia-Hernandez AC, Frey MP, Hollender J, Spaak P. A mixture of environmental organic contaminants in lake sediments affects hatching from Daphnia resting eggs. Environ Toxicol Chem. 2015;34: 338–345. doi:10.1002/etc.2808

64. Putman A. Cryopreservation of Daphnia magna genotypes. 2015. Available: https://lirias.kuleuven.be/1705957?limo=0

65. Brendonck L, De Meester L. Egg banks in freshwater zooplankton: evolutionary and ecological archives in the sediment. Hydrobiologia. 2003;491: 65–84. doi:10.1023/A:1024454905119

66. Decaestecker E, Gaba S, Raeymaekers JAM, Stoks R, Van Kerckhoven L, Ebert D, et al. Host-parasite 'Red Queen' dynamics archived in pond sediment. Nature. 2007;450: 870–873. doi:10.1038/nature06291

67. Cuenca Cambronero M, Orsini L. Resurrection of dormant Daphnia magna: Protocol and applications. J Vis Exp. 2018. doi:10.3791/56637

68. Asaeda T, Acharya K. Application of individual growth and population models of Daphnia pulex to Daphnia magna, Daphnia galeata and Bosmina longirostris. Hydrobiologia. 2000;421: 141–155. doi:10.1023/A:1003955308697

69. Rabus M, Laforsch C. Growing large and bulky in the presence of the enemy: Daphnia magna gradually switches the mode of inducible morphological defences. Funct Ecol. 2011;25: 1137–1143. doi:10.1111/j.1365-2435.2011.01840.x

70. Martínez-Jerónimo F. Description of the individual growth of Daphnia magna (Crustacea: Cladocera) through the von Bertalanffy growth equation. Effect of photoperiod and temperature. Limnology. 2012;13: 65–71. doi:10.1007/s10201-011-0356-2

71. Orsini L, Gilbert D, Podicheti R, Jansen M, Brown JB, Solari OS, et al. Daphnia magna transcriptome by RNA-Seq across 12 environmental stressors. Sci Data. 2016;3: 160030. doi:10.1038/sdata.2016.30

72. Hobaek A, Larsson P. Sex determination in Daphnia magna. Ecology. 1990;71: 2255–2268. doi:10.2307/1938637

73. Routtu J, Hall MD, Albere B, Beisel C, Bergeron R, Chaturvedi A, et al. An SNP-based second-generation genetic map of Daphnia magna and its application to QTL analysis of phenotypic traits. BMC Genomics. 2014;15: 1033. doi:10.1186/1471-2164-15-1033

74. Dukić M, Berner D, Roesti M, Haag CR, Ebert D. A high-density genetic map reveals variation in recombination rate across the genome of

Daphnia magna. BMC Genet. 2016;17: 137. doi:10.1186/s12863-016-0445-7

75. Olmstead AW, Leblanc GA. Juvenoid hormone methyl farnesoate is a sex determinant in the crustacean Daphnia magna. J Exp Zool. 2002;293: 736–739. doi:10.1002/jez.10162

76. Kato Y, Kobayashi K, Oda S, Tatarazako N, Watanabe H, Iguchi T. Sequence divergence and expression of a transformer gene in the branchiopod crustacean, Daphnia magna. Genomics. 2010;95: 160–165. doi:10.1016/j.ygeno.2009.12.005

77. Ignace DD, Dodson SI, Kashian DR. Identification of the critical timing of sex determination in Daphnia magna (Crustacea, Branchiopoda) for use in toxicological studies. Hydrobiologia. 2011;668: 117–123. doi:10.1007/s10750-010-0534-y

78. Toyota K, Miyakawa H, Yamaguchi K, Shigenobu S, Ogino Y, Tatarazako N, et al. NMDA receptor activation upstream of methyl farnesoate signaling for short day-induced male offspring production in the water flea, Daphnia pulex. BMC Genomics. 2015;16: 186. doi:10.1186/s12864-015-1392-9

79. Toyota K, Sato T, Iguchi T, Ohira T. Methyl farnesoate regulatory mechanisms underlying photoperiod-dependent sex determination in the freshwater crustacean <scp> *Daphnia magna* </scp>. J Appl Toxicol. 2020; jat.4035. doi:10.1002/jat.4035

80. Kato Y, Kobayashi K, Watanabe H, Iguchi T. Environmental sex determination in the branchiopod crustacean Daphnia magna: Deep conservation of a Doublesex gene in the sex-determining pathway. Kopp A, editor. PLoS Genet. 2011;7: e1001345. doi:10.1371/journal.pgen.1001345

81. Mohamad Ishak NS, Nong QD, Matsuura T, Kato Y, Watanabe H. Co-option of the bZIP transcription factor Vrille as the activator of Doublesex1

in environmental sex determination of the crustacean Daphnia magna. Desplan C, editor. PLOS Genet. 2017;13: e1006953. doi:10.1371/journal.pgen.1006953

82. Oda S, Tatarazako N, Watanabe H, Morita M, Iguchi T. Production of male neonates in Daphnia magna (Cladocera, Crustacea) exposed to juvenile hormones and their analogs. Chemosphere. 2005;61: 1168–1174. doi:10.1016/j.chemosphere.2005.02.075

83. Mitchell SE. Intersex and male development in Daphnia magna. Hydrobiologia. 2001;442: 145–156. doi:10.1023/A:1017564105942

84. Kato Y, Kobayashi K, Watanabe H, Iguchi T. Introduction of foreign DNA into the water flea, Daphnia magna, by electroporation. Ecotoxicology. 2010;19: 589–592. doi:10.1007/s10646-010-0460-9

85. Kato Y, Shiga Y, Kobayashi K, Tokishita S, Yamagata H, Iguchi T, et al. Development of an RNA interference method in the cladoceran crustacean Daphnia magna. Dev Genes Evol. 2011;220: 337–345. doi:10.1007/s00427-011-0353-9

86. Adhitama N, Matsuura T, Kato Y, Watanabe H. Monitoring ecdysteroid activities using genetically encoded reporter gene in Daphnia magna. Mar Environ Res. 2018;140: 375–381. doi:10.1016/j.marenvres.2018.07.003

87. Nakanishi T, Kato Y, Matsuura T, Watanabe H. CRISPR/Cas-mediated targeted mutagenesis in Daphnia magna. Breuker C, editor. PLoS One. 2014;9: e98363. doi:10.1371/journal.pone.0098363

88. Naitou A, Kato Y, Nakanishi T, Matsuura T, Watanabe H. Heterodimeric TALENs induce targeted heritable mutations in the crustacean Daphnia magna. Biol Open. 2015;4: 364–369. doi:10.1242/bio.20149738

89. Nakanishi T, Kato Y, Matsuura T, Watanabe H. TALEN-mediated homologous recombination in Daphnia magna. Sci Rep. 2016;5: 18312. doi:10.1038/srep18312

90. Nakanishi T, Kato Y, Matsuura T, Watanabe H. TALEN-mediated knock-in via non-homologous end joining in the crustacean Daphnia magna. Sci Rep. 2016;6: 36252. doi:10.1038/srep36252

91. Kumagai H, Nakanishi T, Matsuura T, Kato Y, Watanabe H. CRISPR/Cas-mediated knock-in via non-homologous end-joining in the crustacean Daphnia magna. Lai L, editor. PLoS One. 2017;12: e0186112. doi:10.1371/journal.pone.0186112

92. Rivetti C, Campos B, Piña B, Raldúa D, Kato Y, Watanabe H, et al. Tryptophan hydroxylase (TRH) loss of function mutations induce growth and behavioral defects in Daphnia magna. Sci Rep. 2018;8: 1518. doi:10.1038/s41598-018-19778-0

93. Ismail NIB, Kato Y, Matsuura T, Watanabe H. Generation of white-eyed Daphnia magna mutants lacking scarlet function. Englert C, editor. PLoS One. 2018;13: e0205609. doi:10.1371/journal.pone.0205609

94. Törner K, Nakanishi T, Matsuura T, Kato Y, Watanabe H. Genomic integration and ligand-dependent activation of the human estrogen receptor α in the crustacean Daphnia magna. Shioda T, editor. PLoS One. 2018;13: e0198023. doi:10.1371/journal.pone.0198023

95. Kato Y, Matsuura T, Watanabe H. Genomic integration and germline transmission of plasmid injected into crustacean Daphnia magna eggs. Breuker C, editor. PLoS One. 2012;7: e45318. doi:10.1371/journal.pone.0045318

96. Klüttgen B, Dülmer U, Engels M, Ratte H. ADaM, an artificial freshwater for the culture of zooplankton. Water Res. 1994;28: 743–746. doi:10.1016/0043-1354(94)90157-0

97. Doyle EL, Booher NJ, Standage DS, Voytas DF, Brendel VP, VanDyk JK, et al. TAL Effector-Nucleotide Targeter (TALE-NT) 2.0: tools for TAL effector design and target prediction. Nucleic Acids Res. 2012;40: W117–W122. doi:10.1093/nar/gks608

98. Cermak T, Doyle EL, Christian M, Wang L, Zhang Y, Schmidt C, et al. Efficient design and assembly of custom TALEN and other TAL effector-based constructs for DNA targeting. Nucleic Acids Res. 2011;39: e82–e82. doi:10.1093/nar/gkr218

99. Mittmann B, Ungerer P, Klann M, Stollewerk A, Wolff C. Development and staging of the water flea Daphnia magna (Straus, 1820; Cladocera, Daphniidae) based on morphological landmarks. Evodevo. 2014;5: 12. doi:10.1186/2041-9139-5-12

100. Nong QD, Mohamad Ishak NS, Matsuura T, Kato Y, Watanabe H. Mapping the expression of the sex determining factor Doublesex1 in Daphnia magna using a knock-in reporter. Sci Rep. 2017;7: 13521. doi:10.1038/s41598-017-13730-4

101. Lee G, Hall JC, Park JH. Doublesex gene expression in the central nervous system of Drosophila melanogaster. J Neurogenet. 2002;16: 229–248. doi:10.1080/01677060216292

102. Hempel LU, Oliver B. Sex-specific DoublesexM expression in subsets of Drosophila somatic gonad cells. BMC Dev Biol. 2007;7: 113. doi:10.1186/1471-213X-7-113

103. Robinett CC, Vaughan AG, Knapp J-M, Baker BS. Sex and the single cell. II. There is a time and place for sex. Hawley RS, editor. PLoS Biol. 2010;8: e1000365. doi:10.1371/journal.pbio.1000365

104. Rideout EJ, Dornan AJ, Neville MC, Eadie S, Goodwin SF. Control of sexual differentiation and behavior by the doublesex gene in Drosophila melanogaster. Nat Neurosci. 2010;13: 458–466. doi:10.1038/nn.2515

105. Raymond CS, Kettlewell JR, Hirsch B, Bardwell VJ, Zarkower D. Expression of Dmrt1 in the genital ridge of mouse and chicken embryos suggests a role in vertebrate sexual development. Dev Biol. 1999;215: 208–220. doi:10.1006/dbio.1999.9461

106. Murphy MW, Sarver AL, Rice D, Hatzi K, Ye K, Melnick A, et al. Genome-wide analysis of DNA binding and transcriptional regulation by the mammalian Doublesex homolog DMRT1 in the juvenile testis. Proc Natl Acad Sci. 2010;107: 13360–13365. doi:10.1073/pnas.1006243107

107. Matson CK, Murphy MW, Griswold MD, Yoshida S, Bardwell VJ, Zarkower D. The mammalian Doublesex homolog DMRT1 is a transcriptional gatekeeper that controls the mitosis versus meiosis decision in male germ cells. Dev Cell. 2010;19: 612–624. doi:10.1016/j.devcel.2010.09.010

108. Camara N, Whitworth C, Van Doren M. Chapter 3. The creation of sexual dimorphism in the Drosophila soma. 2008. pp. 65–107. doi:10.1016/S0070-2153(08)00403-1

109. Bénazéraf B, Pourquié O. Formation and Segmentation of the Vertebrate Body Axis. Annu Rev Cell Dev Biol. 2013;29: 1–26. doi:10.1146/annurev-cellbio-101011-155703

110. Akiyama-Oda Y. Early patterning of the spider embryo: a cluster of mesenchymal cells at the cumulus produces Dpp signals received by germ disc epithelial cells. Development. 2003;130: 1735–1747. doi:10.1242/dev.00390

111. De Robertis EM. Spemann's organizer and the self-regulation of embryonic fields. Mech Dev. 2009;126: 925–941. doi:10.1016/j.mod.2009.08.004

112. Martin BL, Kimelman D. Wnt signaling and the evolution of embryonic posterior development. Curr Biol. 2009;19: R215–R219. doi:10.1016/j.cub.2009.01.052

113. Colbourne JK, Pfrender ME, Gilbert D, Thomas WK, Tucker A, Oakley TH, et al. The ecoresponsive genome of Daphnia pulex. Science (80-). 2011;331: 555–561. doi:10.1126/science.1197761

114. Huylmans AK, López Ezquerra A, Parsch J, Cordellier M. De novo

transcriptome assembly and sex-biased gene expression in the cyclical parthenogenetic Daphnia galeata. Genome Biol Evol. 2016;8: 3120–3139. doi:10.1093/gbe/evw221

115. Campos B, Fletcher D, Piña B, Tauler R, Barata C. Differential gene transcription across the life cycle in Daphnia magna using a new all genome custom-made microarray. BMC Genomics. 2018;19: 370. doi:10.1186/s12864-018-4725-7

116. Molinier C, Reisser CMO, Fields P, Ségard A, Galimov Y, Haag CR. Identification of general patterns of sex-biased expression in Daphnia , a genus with environmental sex determination. G3: Genes|Genomes|Genetics. 2018;8: 1523–1533. doi:10.1534/g3.118.200174

117. Doma S. Ephippia of Daphnia magna Straus - A technique for their mass production and quick revival. Hydrobiologia. 1979;67: 183–188. doi:10.1007/BF00126718

118. Davison J. Activation of the ephippial egg of Daphnia pulex. J Gen Physiol. 1969;53: 562–575. doi:10.1085/jgp.53.5.562

119. Kato Y, Kobayashi K, Oda S, Tatarazako N, Watanabe H, Iguchi T. Cloning and characterization of the ecdysone receptor and ultraspiracle protein from the water flea Daphnia magna. J Endocrinol. 2007;193: 183–194. doi:10.1677/JOE-06-0228

120. Major AT, Smith CA. Sex reversal in birds. Sex Dev. 2016;10: 288–300. doi:10.1159/000448365

121. Todd E V., Liu H, Muncaster S, Gemmell NJ. Bending genders: The biology of natural sex change in fish. Sex Dev. 2016;10: 223–241. doi:10.1159/000449297

122. Newell NR, New FN, Dalton JE, McIntyre LM, Arbeitman MN. Neurons that underlie Drosophila melanogaster reproductive behaviors: Detection

of a large male-bias in gene expression in fruitless-expressing neurons. G3 Genes|Genomes|Genetics. 2016;6: 2455–2465. doi:10.1534/g3.115.019265

123. Kato Y, Perez CAG, Mohamad Ishak NS, Nong QD, Sudo Y, Matsuura T, et al. A 5’ UTR-overlapping lncRNA activates the male-determining gene doublesex1 in the crustacean Daphnia magna. Curr Biol. 2018;28: 1811-1817.e4. doi:10.1016/j.cub.2018.04.029

124. An W, Wensink PC. Integrating sex- and tissue-specific regulation within a single Drosophila enhancer. Genes Dev. 1995; 256–266. doi:10.1101/gad.9.2.256

125. Bayrer JR, Zhang W, Weiss MA. Dimerization of Doublesex is mediated by a cryptic Ubiquitin-associated domain fold. J Biol Chem. 2005;280: 32989–32996. doi:10.1074/jbc.M507990200

126. Ghosh N, Bakshi A, Khandelwal R, Rajan SG, Joshi R. The Hox gene Abdominal-B uses DoublesexF as a cofactor to promote neuroblast apoptosis in the Drosophila central nervous system. Development. 2019;146: dev175158. doi:10.1242/dev.175158

127. Siggers T, Gordan R. Protein-DNA binding: complexities and multi-protein codes. Nucleic Acids Res. 2014;42: 2099–2111. doi:10.1093/nar/gkt1112

128. Kochetov A V. Alternative translation start sites and hidden coding potential of eukaryotic mRNAs. BioEssays. 2008;30: 683–691. doi:10.1002/bies.20771

129. Wuerz M, Whyard S, Loadman NL, Wiegand MD, Huebner JD. Sex determination and gene expression in Daphnia magna exposed to juvenile hormone. J Plankton Res. 2019;41: 393–406. doi:10.1093/plankt/fbz025

130. Wang W, Yoder JH. Hox-mediated regulation of doublesex sculpts sex-specific abdomen morphology in Drosophila. Dev Dyn. 2012;241: 1076–1090. doi:10.1002/dvdy.23791

131. Robinson CD, Lourido S, Whelan SP, Dudycha JL, Lynch M, Isern S. Viral transgenesis of embryonic cell cultures from the freshwater microcrustaceandaphnia. J Exp Zool Part A Comp Exp Biol. 2006;305A: 62–67. doi:10.1002/jez.a.250

132. Toyota K, Williams TD, Sato T, Tatarazako N, Iguchi T. Comparative ovarian microarray analysis of juvenile hormone-responsive genes in water flea Daphnia magna: potential targets for toxicity. J Appl Toxicol. 2017;37: 374–381. doi:10.1002/jat.3368

133. Kouno T, Moody J, Kwon AT-J, Shibayama Y, Kato S, Huang Y, et al. C1 CAGE detects transcription start sites and enhancer activity at single-cell resolution. Nat Commun. 2019;10: 360. doi:10.1038/s41467-018-08126-5

134. Reisser CMO, Fasel D, Hürlimann E, Dukič M, Haag-Liautard C, Thuillier V, et al. Transition from environmental to partial genetic sex determination in Daphnia through the evolution of a female-determining incipient W chromosome. Mol Biol Evol. 2016; msw251. doi:10.1093/molbev/msw251

135. Picard MA-L, Cosseau C, Mouahid G, Duval D, Grunau C, Toulza È, et al. The roles of Dmrt (Double sex/Male-abnormal-3 Related Transcription factor) genes in sex determination and differentiation mechanisms: Ubiquity and diversity across the animal kingdom. C R Biol. 2015;338: 451–462. doi:10.1016/j.crvi.2015.04.010

136. Panara V, Budd GE, Janssen R. Phylogenetic analysis and embryonic expression of panarthropod Dmrt genes. Front Zool. 2019;16: 23. doi:10.1186/s12983-019-0322-0

137. Bellefroid EJ, Leclère L, Saulnier A, Keruzore M, Sirakov M, Vervoort M, et al. Expanding roles for the evolutionarily conserved Dmrt sex transcriptional regulators during embryogenesis. Cell Mol Life Sci. 2013;70: 3829–3845. doi:10.1007/s00018-013-1288-2

Supplementary information

Table S1: Primer list	
Primer name	**5’ □ 3’ sequence**
Dsx1_start_left	CGGCTTATCTAAAATGTCGGCCC
Dsx1_start_right	CCCACGGACAATTCTTCAGCG
mCherry_check_F	CTACAAGGTGAAGCTGCGCG
mCherry_check_R	GGTGGTCTTGACCTCAGCGT
Seq_Dsx1Start_L	GAAGGGAAAGCTTCGTACCGA
Seq_Dsx1Start_R	GTGATTGTTGACGCCGAGGA
Seq_mChVector_R(head)	GAAGTTCATCACGCGCTCCC
Seq_mChVector_L(tail)	TTTGTGATGCTCGTCAGGGG
vect_connect_L	CAGGTATCCGGTAAGCGGCA
vect_connect_R	GGTGGTCTTGACCTCAGCGT
right_junc_6kb_L	GAAGGAGAACGTACTGTATTATCGAGGC
right_junc_3kb_alt_R	ATAAAGTTTGGTGTAGGGGAGGATGAGG
mCherry_qPCR_F	CTACGACGCTGAGGTCAAGAC
mCherry_qPCR_R	GGTGTAGTCCTCGTTGTGGG
DmagRPL32-realtime-5	GACCAAAGGGTATTGACAACAGA
DmagRPL32-realtime-3	CCAACTTTTGGCATAAGGTACTG
Dsx1_qPCR_F	GTGGGTCCGTTCATTGCGTC
Dsx1_qPCR_R	GTGGGTCCGTTCATTGCGTC
Dapma7bEVm005257_qPCR_F	TCTAATGCCAGTGCGAAATCC
Dapma7bEVm005257_qPCR_R	CTAAACGCATCTTCCGTCGTC
Dapma7bEVm007306_qPCR_F	GGCCATTCAAACTCAACATCGC
Dapma7bEVm007306_qPCR_R	GGGAAGTGTACGAAAAGCTGGT
Dapma7bEVm016950_qPCR_F	TGGAACGAACTTCAACGACGA
Dapma7bEVm016950_qPCR_R	CGGTAACCACGGCAACCTAC
Dapma7bEVm013357_qPCR_F	GTCAAGAGGATGATGGCGTTCC
Dapma7bEVm013357_qPCR_R	CGTGAGCTGATTCGTCCGTG
Dapma7bEVm016402_qPCR_F	CCAGCGAAAGAGAACACCGTAG
Dapma7bEVm016402_qPCR_R	GGAAGCGAGTTTCACCGAACC
Dapma7bEVm000342_qPCR_F	TCAGGGTCATCGCCAAATCG
Dapma7bEVm000342_qPCR_R	GCCACATTGTAGATCGTCCGT
Dapma7bEVm027428_qPCR_F	CATGAATCTGGGCGGTGCT
Dapma7bEVm027428_qPCR_R	GTGGGTCCGTTCATTGCGTC

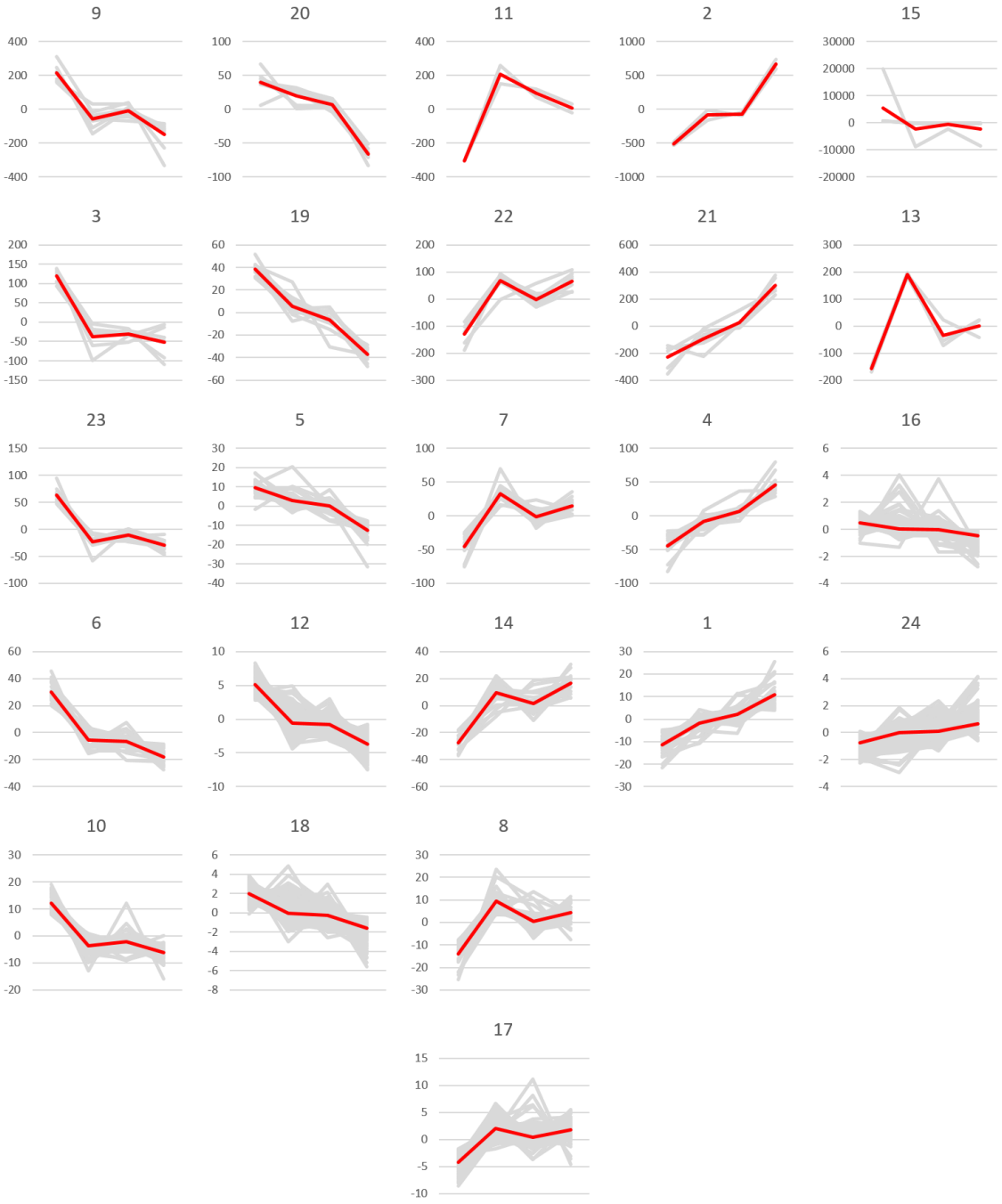

Figure S1A: The same 24 clusters from K-medoid analysis as shown in Figure 3.5. Red line in each cluster indicate the mean value of all genes in that cluster. Cluster names in number are generate by the software during analysis and have no particular meaning.

Figure S1B: Secondary clustering of the 24 clusters in Figure S1A. Note that cluster 13, 15, 16 and 24 were not used due to small difference or non-relatable pattern across samples. First, the expression values of each mean lines were normalized to percentage scale with the lowest values among 4 positions represent 0% and highest values represents 100%. Next, K-mean clustering was performed one more time, resulted in the categorization of these normalized patterns into 4 groups as shown in the figure. In the two binary groups, expression values of Line A male, Line B male and WT male generally fell on the same upper or lower one-third section. In the two non-binary groups, expression values of Line A male and/or Line B male generally fell on the middle one-third section.

List of publications

1. Nong QD, Ishak NS, Matsuura T, Kato Y, Watanabe H. Mapping the expression of the sex determining factor *Doublesex1* in *Daphnia magna* using a knock-in reporter. Scientific reports. 2017 Nov 2;7(1):1-3. doi: 10.1038/s41598-017-13730-4

2. Nong QD, Matsuura T, Kato Y, Watanabe H. Two *Doublesex1* mutants revealed a tunable gene network underlying intersexuality in *Daphnia magna*. PloS one. 2020 Aug 31;15(8):e0238256. doi: 10.1371/journal.pone.0238256

Acknowledgements

This work would never be completed without

My supervisor, Professor Dr. Hajime Watanabe of Department of Biotechnology, Graduate School of Engineering, Osaka University. Thank you for giving me a chance to work under your guidance, and for the patience and kindness to let me freely enjoy life as a scientist at your laboratory.

Associate Professor Dr. Tomoaki Matsuura, who must have officially become Professor by the time I graduate. Thank you for all the scientific advices, as well as your kind concerns during my long staying.

Assistant Professor Dr. Yasuhiko Kato. Your academic support and instructions were more than everything I can ask for from a professor.

Professor Dr. Toshiya Muranaka and Professor Dr. Kohsuke Honda, also from the same department. I am honored and deeply grateful to have you as my reviewers during pre-defense.

Japanese Government and Monbukagakusho Scholarship (MEXT), who was my financial sponsor.

Professor Dr. Yutaka Suzuki of Graduate School of Frontier Sciences, The University of Tokyo, as well as the “先進ゲノム支援” Program, who have offered a great collaboration and support.

My friends and family. I love you.